Plant Cell Advance Publication. Published on February 5, 2020, doi:10.1105/tpc.19.00826

RESEARCH ARTICLE

Persulfidation-based Modification of Cysteine Desulfhydrase and the NADPH Oxidase RBOHD Controls Guard Cell Abscisic Acid Signaling

Jie Shen[1,8], Jing Zhang[1,8], Mingjian Zhou[1,8], Heng Zhou[1,8], Beimi Cui[2], Cecilia Gotor[3], Luis C. Romero[3], Ling Fu[4], Jing Yang[4], Christine Helen Foyer[5,6], Qiaona Pan[2,7], Wenbiao Shen[1], Yanjie Xie[1]

[1] Laboratory Center of Life Sciences, College of Life Sciences, Nanjing Agricultural University, Nanjing 210095, PR China
[2] Institute of Molecular Plant Sciences, University of Edinburgh, Edinburgh EH9 3BF, UK.
[3] Instituto de Bioquímica Vegetal y Fotosíntesis, Consejo Superior de Investigaciones Científicas y Universidad de Sevilla, Avenida Américo Vespucio, 49, 41092 Sevilla, Spain
[4] State Key Laboratory of Proteomics, Beijing Proteome Research Center, National Center for Protein Sciences • Beijing, Beijing Institute of Lifeomics, Beijing 102206, China
[5] Centre for Plant Sciences, Faculty of Biological Sciences, University of Leeds, Leeds, LS2 9JT, UK
[6] School of Biosciences, College of Life and Environmental Sciences, University of Birmingham, B15 2TT, UK
[7] The Key Laboratory of Biotechnology for Medicinal Plant of Jiangsu Province, School of Life Science, Jiangsu Normal University, Xuzhou 221116
[8] These authors contributed equally.
Correspondence yjxie@njau.edu.cn.

Short title: Persulfidation in guard cells

One-sentence summary: A persulfidation-based reversible post-translational modification of cysteine desulfhydrase and NADPH oxidase RBOHD fine-tunes guard cell ABA signaling.

The author responsible for distribution of materials integral to the findings presented in this article in accordance with the policy described in the Instructions for Authors (www.plantcell.org) is: Yanjie Xie; yjxie@njau.edu.cn

ABSTRACT

Hydrogen sulfide (H_2S) is a gaseous signaling molecule that regulates diverse cellular signaling pathways through persulfidation, which involves the post-translational modification of specific cysteine residues to form persulfides. However, the mechanisms that underlie this important redox-based modification remain poorly understood in higher plants. We have, therefore, analyzed how protein persulfidation acts as a specific and reversible signaling mechanism during the abscisic acid (ABA) response in *Arabidopsis thaliana*. Here we show that ABA stimulates the persulfidation of L-CYSTEINE DESULFHYDRASE 1 (DES1), an important endogenous H_2S enzyme, at Cys44 and Cys205 in a redox-dependent manner. Moreover, sustainable H_2S accumulation drives persulfidation of the NADPH oxidase RESPIRATORY BURST OXIDASE HOMOLOG PROTEIN D (RBOHD) at Cys825 and Cys890, enhancing its ability to produce reactive oxygen species. Physiologically, S-persulfidation-induced RBOHD activity is relevant to ABA-induced stomatal closure. Together, these processes form a negative feedback loop that fine-tunes guard cell redox homeostasis and ABA signaling. These findings not only expand our current knowledge of H_2S function in the context of guard cell ABA signaling, but also demonstrate the presence of a rapid signal integration mechanism involving specific and reversible redox-based post-translational modifications that occur in response to changing environmental conditions.

INTRODUCTION

Through evolution and diversification, land plants have adopted robust mechanisms to perceive and relay signals that convey information about water stress. The stomatal aperture in the epidermis of plant leaves is formed by a pair of specialized guard cells, which can sense multiple stimuli and, consequently, control gas exchange and transpirational water loss, which is critical for plant growth and sustenance in stressful and ever-changing

environments (Blatt, 2010; Kim et al., 2010). Importantly, under drought stress, the hyperosmotic signal causes the accumulation of the phytohormone abscisic acid (ABA), which is regulated transcriptionally and post-translationally and integrates into a complex signaling network that regulates stomatal aperture (Zhu et al., 2016).

Reactive oxygen species (ROS) act as second messengers in guard cell responses to most of the stimuli that induce stomatal closure (Wang and Song, 2010). NADPH oxidase (respiratory burst oxidase homolog, RBOH) is a homolog of a mammalian 91 kDa glycoprotein subunit of phagocyte oxidase (gp91*phox*), and a key enzyme in the production of ROS from the outer leaflet of the plasma membrane (Anderson et al., 2011; Marino et al., 2012). Among the ten RBOH genes found in the *Arabidopsis thaliana* genome, the RBOH D and F isoforms play pivotal roles in ROS production, which is rate-limiting to guard cell ABA signal transduction (Kwak et al., 2003). Similarly to mammalian RBOHs, these plant polytopic membrane proteins possess a core C-terminal region containing the functional NADPH-oxidizing dehydrogenase domain responsible for superoxide generation (Suzuki et al., 2011). This C terminus also functions as a toggle switch that affects the access of the NADPH substrate to the enzyme (Magnani et al., 2017). Additionally, plant RBOHs contain an N-terminal intracellular region that carries two EF-hand motifs and a number of phosphorylation sites, which can be activated *via* Ca^{2+} binding and protein phosphorylation events that occur individually or synergistically and involve protein kinases (Marino et al., 2012). Nevertheless, mutagenesis experiments have indicated that Ser343 and Ser347 residues are necessary but not sufficient for elicitor-induced full activation of AtRBOHD (Nuhse et al., 2007). Apart from these canonical post-translational modifications of the N-terminal, the Cys890 amino acid residue in the RBOHD C-terminal is susceptible to modification by nitric oxide, to form a cysteine S-nitrosylation, which suppresses ROS production during the defense response to infection by *Pseudomonas syringae* (Yun et al., 2011). Despite a long-established

correlation between ABA-induced stomatal closure and a ROS burst, through the activation of RBOHD/F, the mechanisms underpinning this activation remain unclear.

Over recent years, tremendous progress has been made in unveiling the biological relevance of hydrogen sulfide (H_2S), a small gaseous molecule that functions as an important developmental and stress-responsive signal in prokaryotes and eukaryotes (Lai et al., 2014; Guo et al., 2016; 2017). H_2S regulates many physiological processes throughout the plant life cycle, including seed dormancy and germination, root growth, cell senescence, autophagy, stomatal aperture/closure, and immunity (Xie et al., 2013; 2014; Aroca et al., 2018; Corpas et al., 2019). H_2S signaling has been implicated in plant stress responses to high salinity, drought, heavy metals, high temperature, osmotic stress, and oxidative stress (Gotor et al., 2019). A considerable number of reports highlight the importance of H_2S and the pathways to its production in plants (Xie et al., 2013; Guo et al., 2016; Gotor et al., 2019; Shen et al., 2019). Although H_2S production occurs predominantly *via* the photosynthetic sulfate-assimilation pathway in chloroplasts, most chloroplastic sulfide dissociates to its ionic form, HS^-, as the pH is basic and H_2S is unable to cross the chloroplast membrane. Therefore, the largest proportion of endogenous cytosolic H_2S is generated from L-cysteine by cysteine-degrading enzymes (Gotor et al, 2019), of which L-cysteine desulfhydrase 1 (DES1) is the first and most characterized (Alvarez et al., 2010). Recently, a number of studies have reported that H_2S produced by DES1 is an important player in guard cell ABA signaling and plant drought tolerance (Garcia-Mata, 2010; Jin et al., 2013; Du et al., 2019). In wheat (*Triticum aestivum*), ABA biosynthesis and signaling are activated by H_2S upon drought stress (Ma et al., 2016). DES1 activity is required for ABA-dependent stomatal closure, and the enzyme acts early in ABA-mediated signal transduction (Scuffi et al., 2014; Du et al., 2019; Zhang et al., 2020). The induction of stomatal closure by sulfurating molecules is impaired in *rbohD* and

rbohF mutants, indicating that NADPH oxidase acts downstream of H_2S in ABA-induced stomatal closure (Scuffi et al., 2018). However, the biochemical and molecular mechanisms by which H_2S regulates downstream targets involved in guard cell ABA signaling have been elusive.

Signaling by H_2S is proposed to occur *via* persulfidation, the post-translational modification of protein cysteine residues (R-SHs) by covalent addition of thiol groups to form persulfides (R-SSHs; Aroca et al., 2018). Similar to but more widespread than S-nitrosylation (Hancock 2019), protein persulfidation is a redox-based modification that regulates diverse physiological and pathological processes. This action provides the framework on which to build an understanding of the physiological effects of H_2S (Paul and Snyder 2012; Filipovic and Jovanović, 2017). The covalent modification that occurs through persulfidation can be reversed by reducing agents such as dithiothreitol (DTT). Persulfidation modulates protein activities by a range of mechanisms, including alterations to subcellular localization, biochemical activity, protein-protein interactions, conformation, and stability (Aroca et al., 2017b; Filipovic et al., 2018). As a typical example of the biological relevance of persulfide modification, increased expression of H_2S-producing enzymes and concomitant H_2S production induce persulfidation of Cys38 in the p65 subunit of NF-κB, which enhances the binding of NF-κB subunits to the co-activator ribosomal protein S3. The activator complex then migrates to the nucleus where it up-regulates the expression of several anti-apoptotic genes (Sen et al., 2012).

In *Arabidopsis thaliana*, a number of persulfidated proteins involved in a variety of biological pathways, have been functionally characterized (Aroca et al., 2015; 2017a; 2018). For instance, H_2S-triggered persulfidation disturbs actin polymerization resulting in stunted root hair growth (Li et al., 2018). Persulfidation regulates the activities of key enzymes involved in the maintenance of ROS homeostasis and redox balance, including ascorbate peroxidase1 and glyceraldehyde 3-phosphate dehydrogenase (GAPDH)

isoform C1 (GAPC1). The nuclear localization of GAPC1 was found to be modulated by DES1-produced H_2S (Aroca et al., 2015; 2017b). Therefore, it is reasonable to infer that the intra-cellular dynamic processes of persulfidation and persulfidation oxidation may be modulated by the redox state in plant cells. The spatio-temporal coordination of H_2S and ROS production is critical to the initiation, amplification, propagation, and containment of H_2S/persulfidation signaling.

In this study, we report the fine-tuned regulation of guard cell redox homeostasis and ABA signaling through persulfidation. In the presence of ABA, DES1 itself was activated by H_2S through persulfidation at Cys44 and Cys205, which led to the transient overproduction of H_2S in guard cells. This could facilitate the over-accumulation of ROS by persulfidation of NADPH oxidase RBOHD on Cys825 and Cys890 residues, thereby inducing stomatal closure. The over-accumulated endogenous ROS may prevent continuously switch on ABA signaling in guard cells, which was achieved by a negative feedback mechanism through persulfide-oxidation of DES1 and RBOHD.

RESULTS

ABA triggers stimulation of activity and persulfidation of DES1

DES1 is a component of the ABA signaling pathway in guard cells and responsible for intracellular H_2S levels and proteome-wide persulfidation (Scuffi et al., 2014; Aroca et al., 2017b; 2018). Proteomic analysis of persulfidated proteins in Arabidopsis leaves showed that DES1 is susceptible to modification by persulfidation (Aroca et al., 2017a). We hypothesize that the activity of DES1 might be regulated by H_2S through persulfidation. To test this possibility, we measured the activities of DES1 recombinant protein treated with either NaHS or DTT followed by dialysis. As expected, NaHS stimulated the enzymatic activity of DES1, indicating that the effects of H_2S on DES activity may rely on the thiol-based redox status (Figure. 1A). Also, DES1

activity was decreased significantly by DTT treatment. To determine whether DES1 is persulfidated in the presence of its product, H_2S, we used a tag-switch assay in which persulfidated cysteine was labeled with cyan-biotin and specifically detected by anti-biotin immune-blot analysis (Angeles et al., 2017; Filipovic et al., 2018; Supplemental Figure 1). NaHS induced persulfidation of DES1 recombinant protein. This was then fully abolished by DTT, which is consistent with the occurrence of a reversible thiol modification (Figure 1A).

To determine whether DES1 could be persulfidated in guard cells, we generated a GFP-tagged DES1 transgenic line *pMYB60:DES1-GFP des1*, in which DES1 was expressed specifically in mature guard cells under the control of the guard cell-specific promoter of the *MYB60* transcription factor (Chater et al., 2015; Zhang et al., 2019; Supplemental Figure 2). Transgenic Arabidopsis plants were treated with a wide range of sulfurating molecules, slow-release H_2S donors or DTT. Subsequently, endogenous persulfidated proteins were labeled with cyano-biotin, and purified with streptavidin beads, which were then immunoblotted with an anti-GFP antibody. DES1-GFP expression was detected with an anti-GFP antibody. Moreover, the labeled enzyme was found to be persulfidated *in vivo*, and further strengthened or fully abolished by a wide range of sulfurating molecules or slow-release H_2S donor concentrations or DTT, respectively (Figure 1B; Supplemental Figure 3). However, there was a low but detectable persulfidation signal found in the GFP itself (Supplemental Figure 4). Next, we investigated whether DES1 was persulfidated during guard cell ABA signaling. Time course results revealed that DES1-SSH formation was promoted in the early stage of the ABA response, i.e., 10 min after initiation of the response, in *pMYB60:DES1 des1* plants, indicating the biological relevance of DES1 persulfidation in guard cell ABA signaling (Figure 1C).

Redox-based regulation of persulfidation and enzymatic activity of DES1

Apart from the alterations of enzyme activity, another feature of the nucleophilicity of persulfides is that they react strongly with two-electron oxidants such as H_2O_2 (Filipovic et al., 2018). Thus, persulfidated proteins undergo oxidation reactions to form perthiosulfenic acids in the presence of excess oxidant (Gotor et al, 2019), thereby reducing the effective level of persulfidated proteins. To determine whether DES1 persulfidated residues can be oxidized in the presence of excess ROS, we analyzed the persulfidated levels of DES1 recombinant protein after treatment with H_2O_2 at a wide range of concentrations. The results demonstrated that H_2O_2 led to a dose-dependent decrease in persulfidation of DES1 recombinant protein *in vitro* (Figure 2A) and DES1-GFP protein in guard cells (Figure 2B), concurrently with a dose-dependent decrease in DES1 recombinant protein activity. Time-dependent oxidation of persulfidated DES1 recombinant protein at both low and high concentrations of H_2O_2 was also observed (Figure 2C; Supplemental Figure 5). The DES1-SSH protein level in guard cells increased by 12.9-fold in the presence of DPI (diphenyleneiodonium; Figure 2D), an inhibitor of plant flavoenzymes, including the ROS-producing enzyme NADPH oxidase, implying that persufidated DES1 might be oxidized by ROS produced from NADPH oxidase. To further verify this possibility, the persulfidation levels of guard cell DES1 proteins were measured in the background of the *RBOHD* mutation, which has been proved to be an important source of ROS in guard cell signaling (Kwak et al., 2003). Under normal conditions, the level of persulfidated DES1 in guard cells was higher in the *rbohD* mutant background than in the parental line *pMYB60:DES1 des1*. Both lines were further enhanced by ABA treatment, indicating that the persulfidation of DES1 was negatively regulated by RBOHD-derived ROS in ABA signaling (Figure 2E). It is plausible that the DES1 on-off switch, controlled by persulfidation and persulfide-oxidation, is reversible. Our time-course experiments revealed that the enhanced persulfidation of DES1 recombinant protein by NaHS

pretreatment was diminished by the application of H_2O_2, and *vice versa* (Figure. 2F-G and Supplemental Figure 6).

Persulfidation of DES1 at Cys44 and Cys205 is a prerequisite for ABA-stimulated activity and stomatal closure

Three cysteine residues in DES1 are putative targets for persulfidation (Cys30, Cys44, and Cys205; Supplemental Figure 7). Mass spectrometric analysis further unequivocally confirmed that C44 and C205 underwent persulfidation in purified recombinant DES1 protein upon NaHS treatment (Figure 3A and B). To determine which cysteine would affect H_2S-mediated persulfidation and the stimulation of DES1 activity, we mutated each cysteine to alanine separately or simultaneously. As shown in Figure 3C and D, two of the mutant proteins, the Cys44Ala and Cys205Ala mutations, significantly lost the inducing effect of NaHS on persulfidation of DES1 recombinant protein, with Cys205Ala presenting dominant function. Meanwhile, the Cys44Ala mutation decreased the level of DES1 recombinant protein persulfidation, which could be partially rescued by treatment with NaHS, but eliminated by the addition of DTT (Supplemental Figure 8). In contrast, following the substitution of Cys205 with alanine, virtually no persulfidation of DES1 recombinant protein was detected, even after NaHS treatment. Subsequently, we prepared protoplasts from plants transiently expressing the different DES1 protein versions fused to GFP and examined the level of pesulfidation of the DES1 mutant proteins *in vivo* (Figure 3E). While DES1-GFP was found to be persulfidated in protoplasts, the amount of persulfidated protein (DES1-GFP-SSH) was reduced partially in protoplasts expressing the mutated version of Cys40Ala and was totally undetectable in Cys205Ala and Cys30/44/205Ala mutants, which was in agreement with the results from the *in vitro* observations of mutant DES1 recombinant protein. Moreover, the formation of DES1-GFP-SSH could be enhanced by ABA or NaHS treatment of wild type plants (Figure 3F).

In this study, we focused on the functional characterization of Cys44 and Cys205, since a mutation at Cys30 did not significantly affect the persulfidation of DES1 recombinant protein. Treatment with NaHS led to marked induction of DES1 recombinant protein activity, but did not affect DES activity in the Cys44/205Ala double mutant and Cys30/44/205Ala triple mutant (Figure 3G). These mutants displayed a slight reduction in DES1 activity when untreated compared with unmutated DES1 recombinant protein. Similarly, treatment with NaHS or DTT did not alter the persulfication of either the Cys44/205Ala or Cys30/44/205Ala mutated versions (Supplemental Figure 8). Taken together, these results indicated that both Cys44 and Cys205 are key to DES1 protein, function and affect persulfidation-induced DES1 activity.

To explore the regulatory role of persulfide-oxidation at Cys residues on the activity of DES1, we further examined the effects of H_2O_2 on its activity. H_2O_2 treatment of wild type DES1 protein pretreated with NaHS resulted in a significant decrease in activity, whereas DES1 activity in the Cys44/205Ala mutant was unchanged (Figure. 3H). This suggests that the two cys residues coordinate to regulate DES1 activity by persulfide-oxidation.

To examine the biological consequences of DES1 persulfidation, the impact of this modification on ABA-induced stomatal closure was investigated. To do this, we generated the transgenic lines *pMYB60:DES1 des1*, in which DES1 and its mutated versions were specifically expressed in mature guard cells. When treated with ABA, guard cells of *pMYB60:DES1 des1*, *pMYB60:DES1*^{Cys30Ala} *des1*, and *pMYB60:DES1*^{Cys44Ala} *des1* plants showed increased H_2S production and stomatal closure, similar to that of the wild type (Figure 3G; H; Supplemental Figure 9). However, these ABA-induced responses were abolished in *pMYB60:DES1*^{Cys205Ala} *des1* and *pMYB60:DES1*$^{Cys44/205Ala}$ *des1* plants (Figure 3I and J). Consistent with this, the ABA treatment time course showed that the guard cell-impaired ABA responses in *pMYB60:DES1*$^{Cys44/205Ala}$ *des1* were similar to those of *des1,*

which can be restored by application of NaHS (Figure 3K, L; and Supplemental Figure 10).

RBOHD-derived ROS in guard cells are genetically required for DES1-regulated stomatal closure

RBOHD is responsible for the auto-propagation wave of ROS production in each cell along its systemic path, which is required for required for system-acquired acclimation (Miller et al., 2009; Mittler et al., 2011; Gilroy et al., 2014). In order to elucidate the tissue-specific function of RBOHD, we expressed RBOHD protein in the *rbohD* background under the control of *ProML1*, *ProCAB3* and *ProMYB60* promoters, which have been used widely to express proteins of interest in epidermal (including guard cells), mesophyll, and guard cells, respectively (Chater et al., 2015; Kirchenbauer et al., 2016; Bernula et al., 2017; Supplemental Figure 11). A stomatal bioassay was conducted using various tissue-specific complementation lines together with corresponding wild type and *rbohD* mutant plants, under ABA, NaHS, or H_2O_2 treatments. Interestingly, the impaired production of ROS triggered by ABA in the guard cells of *rbohD* was rescued when RBOHD was expressed in either epidermal or guard cells (Figure. 4A; upper panel; Supplemental Figure 12). Accordingly, the *rbohD*, stomatal responses of tissue-specific complementation lines were induced by ABA and NaHS (Figure. 4A; lower panel).

Although there were a number of mesophyll cells attached to the strips after peeling, we observed that the mesophyll transgenic line behaved similarly to the guard cell complementation line. Importantly, a significant net ROS-associated influx was found in either ABA- or NaHS-treated guard cell of *pCAB3:RBOHD rbohD* plants, while a small net ROS-associated influx was detected in *rbohD* mutants (Figure 4B). These results suggested that RBOHD activity in both epidermal and mesophyll cells contributed to ABA-induced ROS production in guard cells and, hence, stomatal closure.

Previous pharmacological results showed that stomatal closure was impaired in wild type epidermal strips treated with NaHS in the presence of DPI, an inhibitor of plant flavoenzymes, including the NADPH oxidase, indicating the interplay between H_2S and H_2O_2 (Scuffi et al., 2018). The NADPH oxidase isoforms RBOHD and RBOHF are responsible for the majority of guard cell H_2O_2 production (Kwak et al., 2003). To further evaluate the contribution of RBOHD to H_2S-induced stomatal closure, we crossed *des1* with *rbohD* mutant plants and a homozygous *des1 rbohD* line was identified by genotyping-based PCR (Supplemental Figure 13). Our genetic data further demonstrated that, compared with the *des1* mutant, NaHS-induced ROS production and stomatal closure were almost fully abolished in *des1 rbohD* (Figure 4C), indicating that RBOHD is required genetically for DES1/H_2S-induced stomatal closure. The stomatal response and ROS production within *des1 rbohD* guard cells were less ABA sensitive, but the corresponding responses to H_2O_2 were not altered.

Our results indicated that the regulation between intercellular ROS production and ABA signaling may occur during stomatal closure (Figure 4A-C). To further investigate whether intercellular ROS signaling was regulated by DES1, we expressed RBOHD protein in the *des1 rbohD* background under the control of tissue-specific promoters. ABA treatment failed to induce stomatal closure when RBOHD was expressed in either epidermal, mesophyll, or guard cells of the line carrying the *des1 rbohD* background (Supplemental Figure 14). Together with the results shown in Figure 4A, our observations suggested that functional DES1 activity is involved in ABA-triggered guard cell ROS production and intercellular ROS relay.

H_2S triggered stimulation of NADPH oxidase activity of RBOHD

Next, to examine whether NADPH oxidase activity could be influenced directly by H_2S *in vitro*, we performed enzyme activity assays of NADPH oxidase. Total crude membrane proteins from wild type and *des1* mutant plants were extracted and treated with different concentration of sulfurating molecules,

followed by dialysis, before determination of NADPH oxidase activity. In both wild type and *des1* plants, we clearly observed direct and significant activation of NADPH oxidases by two sulfurating molecules, in a dose-dependent manner (Figure 4D). NADPH oxidase in the *des1* mutant was present in much lower amounts than in the wild type (Col-0) at basal level, suggesting the important role of endogenous H_2S produced by DES1 in regulating NADPH oxidase activity *in vivo*.

To verify the contribution of RBOHD function to H_2S-induced NADPH oxidase, changes to NADPH oxidase activity in the presence or absence of NaHS were determined in a *rbohD* mutant and rescued line *pRBOHD:RBOHD rbohD*. In this case, while low basal levels of NADPH oxidase activity in the *rbohD* mutant were still detectable compared with the wild type (Col-0), the NaHS-induced activity of NADPH oxidase observed in the wild type was almost fully abolished in this mutant (Figure. 4E). This low level of NADPH oxidase activity in the *rbohD* mutant was partially rescued in *pRBOHD:RBOHD rbohD*, indicating the predominant contribution of RBOHD to NaHS-induced NADPH oxidase activity *in vivo*.

ABA induces persulfidation of RBOHD on Cys825 and Cys890

RBOHD protein contains 10 cysteines that might serve as potential sites for persulfidation-based modification by H_2S in the amino-terminal portion (N-terminal; Cys208), carboxy-terminal portion (C-terminal; Cys825 and 890), extracellular portion (Cys410, 412, 432, 651 and 695), and transmembrane portion (Cys387 and 480). To determine whether the cytosolic sides of RBOHD might be persulfidated, the C- and N-terminal portions of this protein were expressed and exposed to sulfurating molecules typically used to score for persulfidation *in vitro.* A tag-switch analysis revealed that persulfidation of the C-terminal portion of RBOHD recombinant protein was induced by two sulfurating molecules individually (Figure 5A), which was in agreement with the results from the analysis of the persulfidation level of RBOHD-C-GFP in

protoplast (Figure 5B; Supplemental Figure 15), and treated with two H_2S donors as well (Supplemental Figure 16). However, no persulfidation of the N-terminal portion was detected, regardless of the addition of sulfurating molecules (Figure 5C).

We next determined whether the RBOHD-C terminal was persulfidated during the plant response to ABA. Following ABA treatment, the level of persulfidated RBOHD-C-SSH protein was increased, but this was largely impaired in *des1* plants, further suggesting a regulatory role for DES1 in modulating the persulfidation the RBOHD C-terminal (Figure. 5D). Subsequently, we analyzed RBOHD-C-SSH formation following treatment with H_2O_2 at a wide range of concentrations. The results suggested that H_2O_2 led to a time and dose- dependent decrease in the persulfidation of RBOHD-C-SSH protein both *in vitro* and *in vivo* (Figure 5E and F; Supplemental Figure 17). The level of RBOHD-C-SSH was consistently higher in the presence DPI, regardless the presence of ABA (Figure 5G). Moreover, similarly to the persulfidation of DES1 recombinant protein, persulfidation and persulfide-oxidation processes were reversible on the thiol groups of RBOHD-C terminal protein (Supplemental Figure 18).

The cysteine residues within the RBOHD-C terminal were, therefore, mutated either individually or in combination and the resulting proteins were expressed, treated with sulfurating molecules, and analyzed by tag-switch assay. Both the mutations of Cys825Ala or Cys890Ala significantly impaired persulfidation of RBOHD-C terminal recombinant protein, particularly Cys825Ala (Figure 5H), but this could be reversed by treatment with two sulfurating molecules, separately (Supplemental Figure 19). Similarly, *in vivo* results demonstrated that persulfidation was additive on Cys825 and Cys890, and was almost completely eliminated in the Cys825/890Ala double mutant, which was not affected by treatments with either ABA or NaHS (Figure 5I-J). Unfortunately, we failed to identify any persulfided sites on RBHOD-C recombinant protein, probably due to the low abundance and/or poor purity of

the purified protein. Collectively, these findings imply that RBOHD is specifically persulfidated at both Cys825 and Cys890, with Cys825 being the preferred target.

The *Arabidopsis thaliana* genome contain 10 genes that encode NADPH oxidase, of which RBOHDA, B, and C contain cysteine residues that are homologous to both Cys825 and Cys890 of RBOHD, indicating that different RBOH proteins might also be persulfidated in this species. We therefore expressed recombinant RBOHC-C terminal mutated versions and exposed them to either NaHS or DTT. As was the case with the RBOHD-C terminal, the unmutated RBOHC-C terminal was specifically persulfidated, but mutations of the conserved cysteines blocked this process from occurring the protein persulfidation (Supplemental Figure 20). The conservation of cysteine residues and the persulfidation-dependent regulation of RBOH family proteins suggest that persulfidation-mediated activation is a general regulatory mechanism adopted by plants.

RBOHD persulfidation controls ABA-stimulated ROS production and stomatal closure

We investigated whether the persulfidation-mediated activation of RBOHD plays a role in ABA-stimulated ROS production and stomatal responses. To explore the possible biological consequences of Cys825 and Cys890 persulfidation on RBOHD activity, we monitored NADPH oxidase activities in mutant *rbohD* plants expressing wild type RBOHD, Cys825Ala, Cys890Ala or Cys825/890Ala driven by the native *RBOHD* promoter (Supplemental Figure 21). NaHS-induced leaf NADPH oxidase activity was significantly impaired in the *pRBOHD:RBOHD*^{Cys825Ala} *rbohD* and *pRBOHD:RBOHD*^{Cys890Ala} *rbohD* lines, compared with *pRBOHD:RBOHD rbohD* (Figure 6A). Inducible NADPH oxidase activity and ROS accumulation in guard cells were fully abolished in the *pRBOHD:RBOHD*$^{Cys825/890Ala}$ *rbohD* line, implying an additive effect of RBOHD persulfidation at Cys825 and C890 during ABA/H_2S-triggered NADPH

oxidase activity, which results in increased ROS generation in guard cells (Figure 6B, upper panel).

Next, we analyzed the responsiveness of the transgenic *rbohD* lines (expressing either wild type *RBOHD* or mutant derivatives) to ABA or NaHS during stomatal responses. When treated with NaHS or ABA, *pRBOHD:RBOHD rbohD* exhibited stomatal closure similar to that of the wild type (Figure 6B lower panel). However, this inducible stomatal closure was markedly reduced in the *pRBOHD:RBOHD*^{Cys825Ala} *rbohD,* *pRBOHD:RBOHD*^{Cys890Ala} *rbohD,* and *pRBOHD:RBOHD*$^{Cys825/890Ala}$ *rbohD* lines.

To confirm that ABA-activated RBOHD function in stomatal closure and ROS production in guard cells are consequences of DES1-triggered persulfidation, we introduced *RBOHD* and its substitutional mutant derivatives under the control of the native *RBOHD* promoter into the *des1 rbohD* mutant, and tested the ROS production and guard cell responses to either ABA or NaHS in the resulting transgenic plants. All of the transgenic plants with the *des1 rbohD* background exhibited reduced ROS production and stomatal responses to ABA, which further reinforces the conclusion that DES1 is genetically required for ABA-induced RBOHD activation and stomatal closure (Figure 6C). When treated with NaHS, *pRBOHD:RBOHD des1 rbohD* guard cells exhibited an increase in ROS and stomatal closure, similar to that of the wild type. However, NaHS-induced ROS activation and stomatal closure were abolished in *pRBOHD:RBOHD*^{Cys825Ala} *des1 rbohD, pRBOHD:RBOHD*^{Cys890Ala} *des1 rbohD,* and *pRBOHD:RBOHD*$^{Cys825/890Ala}$ *des1 rbohD* plants. Collectively, these results suggested that DES1/H_2S-triggered RBOHD persulfidation at Cys825 and Cys890 plays a critical role in modulating ABA-induced guard cell ROS production and stomatal closure.

DISCUSSION

In dry conditions, plants rapidly synthesize the drought stress hormone ABA at high levels to trigger signal transduction events that lead to stomatal closure and reduced water loss. Although ABA is known to activate stress responses, the mechanisms by which ABA signals are relayed in guard cells remain unresolved. In this study, we unraveled the molecular framework for DES1/H_2S-triggered protein persulfidation, which links ABA signaling pathways with stomatal closure.

Persulfidation of DES1 and RBOHD during ABA-induced stomatal closure

Maintaining the redox status is a conspicuous feature of signaling cascades and precisely controlled in plant cells (Smirnoff and Arnaud 2019; Hancock 2019). Interestingly, the reducing and oxidizing molecules H_2S and H_2O_2, which are generated by DES1 and NADPH oxidase, are both critically involved in the ABA response (Kwak et al., 2003; Scuffi et al., 2018). However, the molecular mechanisms that mediate the synthesis and function of these signaling molecules are poorly understood. Perhaps the best example of the convergent action of DES1 and NADPH oxidase is the control of stomatal aperture, where H_2S is suggested to serve as a gasotransmitter in stomatal closure (Honda et al., 2015; Papanatsiou et al., 2015). Our data are entirely consistent with these observations (Scuffi et al., 2018). While closure was not evident in the *des1 rbohD* mutant line following treatment with NaHS, the guard cell response to H_2O_2 was the same as that of wild type. The impairment in ABA/NaHS sensitivity of *des1 rbohD*, in terms of stomatal closure, was not altered by the introduction of *DES1* driven by guard cell promoter *MYB60*, which illustrated a positive regulatory role for RBOHD downstream of DES1/H_2S in guard cell ABA signaling. RBOHD was shown to mediate long-distance signaling via a dynamic auto-propagating wave of ROS that can travel at a rate of up to 8.4 cm min^{-1} through the apoplast (Miller et al., 2009). In support of this finding, both ABA and NaHS triggered a ROS-associated

influx into guard cells and stomatal closure when RBOHD was tissue-specifically expressed in the *rbohD* mutant background. Our results infer that plants retain the ability to produce ROS signals by RBOHD and facilitate cell-to-cell communications to trigger downstream events in guard cells in response to environmental changes.

H_2S physiologically persulfidates a diverse range of proteins. As persulfidation occurs frequently, this posttranslational modification has been proposed to affect a variety of biological pathways (Aroca et al., 2017; 2018). Here, we demonstrated that ABA-activated DES1-endogenous H_2S physiologically persulfidated DES1 to regulate its activity, with Cys44 and Cys205 as the main sites of this modification. Our results revealed that the activity of persulfidated DES1 can return to the basal state quickly, depending on the dynamic redox status, e.g. endogenous H_2O_2 homeostasis, which can lead to reversible persulfide-oxidation of persulfidated DES1, thus fine-tuning the strength and duration of the ABA signal. Therefore, ROS accumulation may function as a negative feedback mechanism to prevent the continuous triggering of ABA signaling in guard cells, which is achieved by persulfide-oxidation of persulfidated DES1. Moreover, persulfides may serve a protective function of protein thiols in highly oxidized environments (Gotor et al., 2019). It is therefore a matter of importance as DES1-produced H_2S contributes far more to the ABA signaling than previously imagined. The regulatory mechanism is physiologically related to the guard cell ABA response. In *pMYB60:DES1*$^{Cys44/205Ala}$ *des1*, ABA was less effective in inducing guard cell H_2S production and stomatal closure than in wild type plants within the treatment period. This observation supports a positive regulatory role for ABA in the persulfidation and activation of DES1, which may facilitate the downstream H_2S sensing, that is essential in relaying the guard cell ABA signals.

The rapid production of ROS in guard cells acts as systemic secondary messenger to trigger stomatal closure (Song et al., 2013). Plant NADPH

oxidases belong to the RBOH family, and catalyze the production of superoxide that can then be converted into H_2O_2 spontaneously or by superoxide dismutase or peroxidases (Smirnoff and Arnaud 2019). In many cases, RBOHs regulation occurs on the N-terminal extension that carries EF-hand motifs and potential phospho-sites through Ca^{2+} binding and phosphorylation, which are thought to be important for activation of NADPH oxidase (Ogasawara et al. 2008; Chen et al. 2017). Notwithstanding the long-established correlation between ABA signaling and ROS burst activation in guard cells, the mechanisms that underpin the activation of a ROS burst, and are associated with the RBOHD C-terminal, are largely unknown. In this study, we discovered that H_2S regulates guard cell ABA signaling through persulfidation of two cysteines in the C-terminal of RBOHD. Persulfidation triggers RBOHD to facilitate a burst of ROS, which, in turn, causes stomatal closure. This might represent a mechanism for raised ABA-triggered ROS signaling in guard cells. *des1* plants showed reduced NADPH oxidase activity and low persulfidation at the C-terminal of RBOHD, supporting a positive regulatory role for H_2S in the ABA-activated RBOHD.

Our findings are reminiscent of those in plant immunity, where S-nitrosylation at a conserved cysteine (890, not 825) in RBOHD promotes cell death during plant immune function (Yun et al., 2011). While S-nitrosylation on C890 disrupts the side-chain position of Phe921, impeding FAD binding affinity, persulfidation enhances the reactivity of the Cys890 thiol, may render it more nucleophilic, and thus may facilitate its binding with FAD. Importantly, under our conditions, Cys825 was predominantly persulfidated and additional effects of Cys825 and Cys890 on guard cell ROS production and responses were seen. Thus, we could not fully reject the hypothesis that nitrosylation of Cys890 affects the guard cell response. Further investigations using the RBOHD native protein and 3D structure will help to unveil the mechanisms of persulfidation-regulated RBOHD activity. Notably, we observed that the $RBOHD^{Cys825/890Ala}$ mutation abolished the H_2S and ABA responses,

suggesting that the persulfidation of RBOHD plays a regulatory role in guard cell ABA responses. It has been reported that persulfidation precedes nitrosylation on the same cysteine residue in several instances (Sen et al., 2012; Vandiver et al., 2013). This opens the possibility of crosstalk between persulfidation and nitrosylation in the regulation of ROS production and ABA signaling in guard cells. Further clarification of the temporary sequences of persulfidation and nitrosylation would offer new insights into the sophisticated mechanisms of ABA-controlled guard cell signaling.

Redox-based reversible persulfidation controls guard cell ABA signaling

The on-off switch for RBOHD function controlled by persulfidation and persulfide-oxidation may fine-tune the strength or duration of RBOHD activation and ROS signals in response to ABA. Our results indicate that H_2S and ROS produced by DES1 and RBOHD, respectively, can fulfill this role. Although the kinetic and structural details of DES1/RBOHD persulfidation and persulfide-oxidation remain limited, our findings suggest the following: ABA causes rapid and strong activation of DES1 in guard cells, which can persulfidate downstream functional proteins including itself on Cys44 and Cys205, thus amplifying guard cell ABA signals. The inducible DES1/H_2S also persulfidates NADPH oxidase RBOHD on Cys825 and Cys890 to facilitate the rapid induction of a ROS burst and stomatal closure (Figure 7 and the graphic abstract). When ROS accumulate, it triggers persulfide-oxidation of RBOHD and DES1 to form perthiosulfenic acid, leading to ABA de-sensitivity. The reducible S-S bond present in the formed perthiosulfenated Cys can be reduced by disulfide reductases such as thioredoxin, which has been demonstrated in the formed S-sulfocysteine bond in the active site of 3’-phosphoadenosine-5’-phosphosulfate reductase (Palde and Carroll, 2015) The stimulated RBOHD activity may be returned to the basal state quickly through this redox-based posttranslational modification, based on dynamic redox homeostasis. The finding that ROS-triggered persulfide-oxidation of

604 persulfidated RBOHD and DES1 suggests that plants possess yin and yang
605 mechanisms to orchestrate redox signaling coupled with hormonal response,
606 which may feedback to prevent the continual activation of ABA signals in guard
607 cells. As H_2S and ROS are ubiquitous, this yin and yang interplay is most likely
608 to be a rapid regulatory mechanism that primes the paradigmatic
609 ABA-triggered regulation of plant RBOHs and ROS production in guard cells.
610 Correspondingly, tipping the DES1/H2S-RBOHD/ROS balance towards
611 increased endogenous ROS production can trigger protein persulfidation
612 oxidation, further leading these activated proteins to return to their basal states.
613 Plants endowed with this negative feed-back loop could sense the redox status
614 and control ROS homeostasis under ever-changing environments.

615

616 **METHODS**

617 **Plant materials and growth conditions**

618 The Arabidopsis (*Arabidopsis thaliana*) *des1* (SALK_103855; Col-0) mutant
619 was obtained from the Arabidopsis Biological Resource Center
620 (http://www.arabidopsis.org/abrc), *rbohD* was a gift from Prof Wenhua Zhang,
621 Department of Plant Science, Nanjing Agricultural University.

622 The *des1 rbohD* double mutant line was obtained by crossing *rbohD*, with
623 *des1* (Supplemental data set 1). Homozygous mutants were identified by
624 sequencing, combined with PCR-based genotyping and corresponding
625 phenotypes (including reduced plant size and vigor).

626 Seeds were surface sterilized and washed three times with sterile water for
627 20 min, then cultured in petri dishes on solid 1/2 strength MS medium (pH 5.8).
628 Plants were grown in a growth chamber with a 16/8 h (23°C/18°C) day/night
629 regime using bulb type fluorescent light at a light intensity of 100 μmol photons
630 m^{-2} s^{-1} irradiation.

631

632 **Molecular cloning**

1. For expression in *E. coli*

PCR-amplified fragments of At*RBOHD*-N (1-1068 bp), At*RBOHD*-C (2269-2763 bp) and full-length At*DES1* were introduced into PET28a vector (for His fusion) using homologous recombination technique (Vazyme), with the enzyme digestion site of *Nde*I and *Xho*I.

Site-directed mutagenesis was carried out with Mut Express II Fast Mutagenesis Kit (Vazyme). All procedures followed the manufacturer's manual. The specific primers used for AtRBOHD-N, RBOHD-C and full-length At*DES1* are listed in Supplemental data set 1.

2. For transient expression in Arabidopsis protoplasts

PCR-amplified fragments were cloned into PAN580 vector (from AYing Zhang's lab, college of life sciences, Nanjing Agricultural University) at the sides of *Xba*I and *Bam*HI using homologous recombination technique (Vazyme).

Arabidopsis protoplasts were isolated according to the method described previously (Yoo et al. 2007). The transient expression vector PAN580 was delivered into Arabidopsis protoplasts using a PEG-calcium-mediated approach and protoplasts were cultured for 12 h. Protoplasts expressing the targeted GFP driven by the constitutive 35S enhancer under fluorescence microscopy are used for transient expression analysis.

3. For expression in planta

Promoter cloning of *CAB3*, *ML1*, *MYB60*, *RBOHD*. By using Arabidopsis wild type DNA as template, the promoter regions of *CAB3* (2000bp), *ML1* (1500bp), *MYB60* (1500bp), and *RBOHD* (1500bp) were amplified by PCR (Supplemental Data set S1, 2). *CAB3*, *pML1*, *MYB60* fragments were cloned into pCAMBIA 1305 vector (from Aying Zhang's lab, College of life sciences, Nanjing Agricultural University). The *RBOHD* products were cloned into 130221-flag vector (from Yiqun Bao's lab, College of life sciences, Nanjing Agricultural University).

The constructed plasmids were transferred into *Agrobacterium*

tumefaciens strain, and then the inflorescence of Arabidopsis thaliana was infected by dipping. Transgenic plants were selected on 1/2 MS medium containing Hygromycin B (50 ug/ml). Identification of transgenic plants were conducted by genotyping combined with PCR, fluorescence observation and immunoblot analysis.

Expression and purification of recombinant protein

Expression and purification of the recombinant protein were performed in BL21 cells (Vazyme). The 0.1mM IPTG was added, when the bacteria grow to OD_{600}= 0.4-0.6, for 12 h at 16°C. After enriching the bacterial solution, the precipitation was suspended in PBS buffer, the protein was broken by ultrasonic crusher, and then centrifuged at 12000g for 30 min. Take the extract for purification. The HIS-tagged proteins were purified using a NI-NTA pre-packed gravity column (Sangon Biotech), the procedure for protein purification is carried out in accordance with this column specification.

Direct MS analysis of persulfidated cysteine sites on DES1

Direct MS analysis of persulfidated cysteine sites on DES1 was performed as previously described with modifications (Bogdandi et al., 2019; Fu et al., 2019). In brief, purified recombinant proteins (~ 0.1 mg/ml, 120 µL) in 50 mM HEPES, pH 7.6 were incubated with 1mM NaHS at room temperature for 1 hr. Protein samples were then alkylated with IAM (10 mM) in the dark at room temperature for 30 min. Next, alkylated proteins were resolved by SDS-PAGE gel and stained with Coomassie Brilliant Blue. Gel bands corresponding to DES1 (~ 40 kd) were sliced, destained with 50 mM NH_4HCO_3 in 40 % methanol, and subjected to in-gel digestion as previously described (Shevchenko et al., 2006). The resulting peptides were extracted, desalted and evaporated to dryness until LC-MS/MS analysis. LC-MS/MS was performed with the same settings as previously described (Akter et al., 2018, Huang et al., 2019) on a Q Exactive plus (Thermo Scientific) instrument

operated with an Easy-nLC1000 system (Thermo Scientific). The resulting MS data were searched against the protein sequence of DES1 (UniProt accession number: F4K5T2) using pFind 3(Chi et al., 2018). The precursor-ion mass and fragmentation tolerance were 10 p.p.m. and 20 p.p.m., respectively. A specific-tryptic search was used with a maximum of three missed cleavages allowed. Mass shifts of + 15.9949 Da (methionine oxidation, M), + 57.0214 Da ($C_2H_3N_1O_1$, carbamidomethylation, C) and + 88.9935 Da ($C_2H_3N_1O_1S_1$, IAM-derivatized persulfide, C) were searched as for dynamic modifications.

Enzyme activity assay of DES1 recombinant protein

The DES activity for DES1 were determined using the methods described previously (Álvarez et al., 2010). The DES activity was measured by the monitoring the release of sulfide from L-cysteine in a total volume of 3 ml containing, 0.8 mM L-cysteine, 100 mM Tris-HCl (pH9.0), and 300 μL purified DES1 protein. The reaction was initiated by adding L-cysteine. After incubation at 37°C for 15 min, the reaction was terminated by the addition of 300 μl of 30 mM $FeCl_3$ dissolved in 1.2 M HCl and 300 μl 20 mM *N,N*-dimethyl-*p*-phenylenediamine dihydrochloride dissolved in 7.2 M HCl. The formation of methylene blue was determined at 670 nm in a spectrophotometer. The DES enzymatic activity was calculated by comparison to a standard curve of Na_2S. The amount of total protein was determined by the method of Bradford (Bradford, 1976).

SDS-PAGE and Immunoblotting

Protein extracts were separated by 12% SDS-PAGE. After electrophoresis, the gel was transferred to a polyvinylidene difluoride (PVDF) membrane (Roche) at 100 V 45 min at 4°C. The membrane was blocked with 5% skimmed in blocking solution (5% BSA in TBS with 0.5% [v/v] Tween-20) and incubated for 2 h with shaking at room temperature or overnight at 4°C. Immunoblot analysis was performed with antibodies (Supplemental Data Set 2) diluted in blocking

solution at the following dilutions: anti-GFP-HRP-DirecT (MBL), 1:4000; anti-biotin-HRP (abcam), 1:10000. For quantification of protein abundance, ImageJ was used and signals from two independent experiments were quantified. Full-sized membrane scans are presented in Supplemental Figure 22.

Immunochemical detection of S-persulfidated proteins

S-persulfidated proteins were detected using a modified Tag-switch method as described (Aroca et al., 2017).

For *in vitro* assays, the purified recombinant proteins were treated with NaHS, DTT or H_2O_2 at the indicated concentrations, respectively. The proteins were blocked with MSBT, and the S-persulfidated cysteines were labeled by CN-biotin. The S-persulfidated proteins were detected by immunoblot using an anti-biotin antibody (anti-biotin-HRP (abcam), 1:10000).

For *in vivo* assay, Arabidopsis leaves (~1g) were ground in a mortar under liquid nitrogen. Extract and Arabidopsis protoplasts were homogenized in buffer (25 mM TRIS, 100 mM NaCl, 0.2 % Triton X-100, at a pH of 8.0) containing a complete protease inhibitor cocktail (Sigma Aldrich). The extract was centrifuged at 4 °C for 30 min. Blocking buffer 50mM MSBT which dissolved in THF was added to the extract and the solution was incubated at 37°C for 1hr to block free sulfhydryl groups. Proteins was precipitated with acetone and resuspended pellet in buffer (50mM TRIS, 2.5% SDS, 20 mM CN-biotin, at a pH of 8.0) and incubated 3-4 hr 37ºC. Protein was precipitated with acetone, washed with acetone 70% twice, and resuspended pellet in buffer (50mM TRIS, 0.5% SDS, at a pH of 8.0). The biotinylated proteins were purified by immunoprecipitation for 1 h at 25 ºC with 80 µl of streptavidin magnetic particles (Roche). Particles were washed three times and bound proteins were eluted with a suitable buffer, and separated by 12% SDS-PAGE, transferred to a polyvinylidene fluoride membrane. Proteins was detected with an antibody against GFP (anti-GFP-HRP-DirecT; 1:4000; MBL).

753

754 **Measurement of H_2S and ROS in guard cells and stomatal aperture**

755 Epidermal strips of each ecotype were preincubated for 3 h in opening buffer
756 (10 mM MES, pH 6.15, and 50 mM KCl) under light (100 μE $m^{-2}s^{-1}$) and
757 loaded with 7-Azido-4-methylcoumarin (a fluorogenic probe useful for the
758 detection of hydrogen sulfide; Sigma-Aldrich) for 20 min, or loaded with
759 2',7'-Dichlorofluorescin diacetate (H_2DCF-DA; an oxidation-sensitive
760 fluorescent probe to measure ROS; Sigma-Aldrich) for 15 min before washing
761 in MES buffer three times for 15 min each, subsequently treated for 1 h with 10
762 μM ABA, 100 μM NaHS (the sulfurating molecule) or 10 μM H_2O_2 and then
763 analyzed using a TCS-SP2 laser scanning confocal microscope (LSCM; Leica,
764 excitation at 405 nm, emission at 454-500 nm for the detection of hydrogen
765 sulfide; excitation at 488 nm, emission at 500–530 nm for the detection of
766 ROS). Stomatal aperture measurements were carried out as described
767 previously (Xie et al. 2016), epidermal strips were soaked in to the opening
768 buffer ,10 μM ABA, 100 μM HT (the scavenger of H_2S), 100 μM NaHS (the
769 sulfurating molecule) or 10 μM ABA+100 μM HT (the scavenger of H_2S) for 1 h.
770 All manipulations were performed at 25 ±1 °C. Data were analyzed by using
771 ImageJ software. Each value represents the mean of at least 90 stomata taken
772 from different leaves, bars (when present) represent the SE of each treatment.

773

774 **Non-invasive micro-test technique (NMT) measurement**

775 The basic principles of NMT measurement are described (Newman, 2001).
776 The net guard cells ROS-associated fluxes were measured using the
777 Scanning Ion-Selective Electrode Technique system (BIO-001A, Younger USA
778 Sci. & Tech. Corp., Amherst, MA, USA). A ROS-sensitive microsensor was
779 purchased from Xuyue Beijing NMT Service Center. The experimental voltage
780 is +600 mV. The primary position (M1) of ROS-sensitive microsensor was
781 placed 10 μm from the guard cells surface, and further away position (M2) is
782 45 μm. Net guard cell ROS-associated fluxes were calculated by Fick's law of

diffusion: *J* (pmol/cm^2/s)=-*Do*× (*dc*/*dx*), where *Do* indicates the diffusion constant, *dc* the concentration gradient (calibration with H_2O_2 standard curve), and *dx* the distance (30 μm). Experiments were conducted at room temperature (24±1℃) under ambient light. Data (means ± SD, n = 6). Leaves from 1-month-old plant were placed in a Petri dish and immersed in MES (pH 6.15) assay solution, after pre-conditioning, steady-state ion fluxes were recorded over a period of 5 min. Then, an ABA/NaHS-containing stock solution was applied and mixed to reach the required final concentration of 10 μM and 100 μM, respectively.

Determination of NADPH oxidase activity

Crude membrane extracts were isolated according to the method of Wang et al. 1985. 2 g of leaf tissues were ground in liquid nitrogen and dissolved in four volumes of the extraction buffer (25 mM HEPES, pH 7.5, 5 mM EDTA, 2 mM EGTA, 1 mM dithiothreitol, 150 mM KCl, 250 mM mannitol and, 0.5mM PMSF). The crude extract was filtered with four layers of gauze and centrifuged at 10,000g for 20 min and the resulting supernatant was ultra-centrifuged at 50,000g for 30 min. The resulting pellet was resuspended in suspension buffer (2.5mM HEPES, pH 7.5, 5 mM EDTA, 1 mM dithiothreitol, 150 mM KCl, 250 mM mannitol and 1mM PMSF), and used as the membrane fraction to measure NADPH oxidase activity.

The NADPH-dependent O_2^- generating activity in isolated crude membrane was determined by following the reduction of sodium, 3’-[1-[phenylamino-carbonyl]-3,4-tetrazolium]-bis(4-methoxy-6-nitro) benzenesulfonic acid hydrate (XTT) by O_2^- (Sagi and Fluhr 2001). The assay mixture of 1 ml contained 50 mM Tris–HCl buffer (pH 7.5), 0.5 mM XTT, 100 μM NADPH and 15–20 μg of membrane proteins. The reaction was initiated with the addition of NADPH, and XTT reduction was determined at 470 nm. Corrections were done for background production in the presence of 50 units

812 SOD. Rates of O_2^- generation were calculated using an extinction coefficient of
813 2.16×10^4 M^{-1} cm^{-1}.
814
815 **Statistical analysis**
816 Statistical analysis and plotting of graphs were performed using SPSS 16.0. To
817 determine statistical significance, we used one-way or two-way ANOVA
818 (corrected with post-hoc Tukey's HSD test). Differences were considered
819 significant at $P < 0.05$. Statistical data are provided in Supplemental Data Set
820 3.
821
822 **Accession Numbers**
823 DNA and derived protein sequence data from this article are in the Arabidopsis
824 Genome Initiative database under the following accession numbers: *DES1*
825 (At5g28030), *RBOHD* (At5g47910), *RBOHF* (At1g64060), *MYB60*
826 (At1g08810), *ML1* (At5g61960), *CAB3* (At1g29910).
827
828 **Supplemental Data**
829 **Supplemental Figure 1** Analysis of persulfidation of DES1-GFP *in vivo*
830 (Supports **Figure 1**).
831
832 **Supplemental Figure 2** Relative expression of *DES1* in wild type (Col-0),
833 *des1* and lines expressing either a wild type DES1 or Cys30Ala, Cys44Ala,
834 Cys205Ala and Cys30/44/205Ala mutant derivatives driven by *MYB60*
835 promoter (Supports **Figure 1 and 3**).
836
837 **Supplemental Figure 3.** Detection of persulfidation of the DES1 protein *in*
838 *vivo* (Supports **Figure 1**).
839
840 **Supplemental Figure 4.** Analysis of persulfidation of DES1-GFP *in vivo*
841 (Supports **Figure 1**).

Supplemental Figure 5. Time-dependent persulfidation oxidation of DES1-His recombinant protein (Supports **Figure 2**).

Supplemental Figure 6. Persulfidation of DES1-His recombinant protein by H_2O_2 pretreatment (Supports **Figure 2**).

Supplemental Figure 7. Amino acid sequence of DES1 protein. DES1 protein has 323 amino acids in total (Supports **Figure 3**).

Supplemental Figure 8. The persulfidation formation of DES1-His recombinant protein and its derivatives Cys44Ala, Cys205Ala, Cys44/205Ala, and Cys30/44/205Ala (Supports **Figure 3**).

Supplemental Figure 9. Representative images of ABA on the guard cell H_2S production of *des1* rescued lines shown in Figure 3G (Supports **Figure 3**).

Supplemental Figure 10. The effects of NaHS on the guard cell H_2S production (A) and stomatal closure (B) of wild type, *des1*, and *des1* rescued lines (Supports **Figure 3**).

Supplemental Figure 11 Relative expression of *RBOHD* in wild type (Col-0), *rbohD* and lines expressing *RBOHD* under the control of tissue-specific promoters, in which *RBOHD* was expressed in mesophyll cells (*pCAB3:RBOHD*), epidermal (*pML1:RBOHD*), or guard cells (*pMYB60:RBOHD*) individually (Supports **Figure 4**).

Supplemental Figure 12. Representative images of guard cell ROS production for *rbohD* and its rescued lines shown in Figure 4A (Supports

Figure 4).

Supplemental Figure 13. Genotyping for the *des1 rbohD* mutant (Supports **Figure 4**).

Supplemental Figure 14. Stomatal responses of wild type, *des1 rbohD*, and *des1 rbohD* rescued lines (Supports **Figure 4**).

Supplemental Figure 15 Subcellular Localization of RBOHD-C-GFP (Supports **Figure 5**).

Supplemental Figure 16 Detection for the persulfidation of the RBOHD-C terminal *in vivo* (Supports **Figure 5**).

Supplemental Figure 17. A time-dependent decrease of persulfidation of RBOHD-C recombinant protein *in vitro* (Supports **Figure 5**).

Supplemental Figure 18. Reversible persulfidation of RBOHD-C recombinant protein *in vitro* (Supports **Figure 5**).

Supplemental Figure 19. Persulfidation of RBOHD-C recombinant protein and relative derivatives (Supports **Figure 5**).

Supplemental Figure 20. Persulfidation of the RBOHC-C recombinant proteins and related derivatives (Supports **Figure 5**).

Supplemental Figure 21. Relative expression of *RBOHD* in wild type (Col-0), *rbohD* and lines expressing either a wild type RBOHD or Cys825Ala, Cys890Ala and Cys825/890Ala mutant derivatives driven by its native promoter individually (Supports **Figure 6**).

Supplemental Figure 22. Immunoblot membrane scans for this study (Supports **Figure 1-3, and 5**).

Supplemental Data Set 1. Oligonucleotide primers used in this study.

Supplemental Data Set 2. Materials used in this study.

Supplemental Data Set 3. Detailed statistical analyses of the results in this study.

Acknowledgments

The work was supported by grants from the National Natural Science Foundation of China (31670255, 21922702), the Fundamental Research Funds for the Central Universities (KYZ201859), and the National Natural Science Foundation of Jiangsu Province (BK20161447), and the European Regional Development Fund through the Agencia Estatal de Investigación of Spain (grant No. BIO2016-76633-P). The authors wish to thank Prof. Honghong Wu from Huazhong Agricultural University for his helpful advice in NMT experiment. Y.X. wishes to thank his wife Dan Chen, daughter Mengmeng, and family for their unwavering support and encouragement, without which this paper could not have been published.

Author Contributions

J.S., J.Z., H.Z., B.C., J.Y., and Y.X., designed the study. J.S., J.Z., M.Z., H.Z., and L.F., performed the experiments. B.C., Q.P., C.G., L.C.R., L.F., J.Y., W.S., and Y.X. analyzed the data. C.G., L.C.R., C.H.F., and Y.X. wrote the paper.

References

930 Akter, S., L. Fu, Y. Jung, M. L. Conte, J. R. Lawson, W. T. Lowther, R. Sun, K. Liu, J. Yang
931 and K. S. Carroll (2018). Chemical proteomics reveals new targets of cysteine sulfinic acid
932 reductase. Nat Chem Biol *14*, 995-1004.

933 Álvarez, C., Calo, L., Romero, L.C., García, I., and Gotor, C. (2010). An
934 O-acetytlserine(thiol)lyase homolog with L-cysteine desulfhydrase activity regulates
935 cysteine homeostasis in Arabidopsis. Plant Physiol. *152*, 656-669.

936 Anderson, A., Bothwell, J. H., Laohavisit, A., Smith, A. G., and Davies, J. M. (2011). Nox
937 or not? Evidence for algal NADPH oxidases. Trends Plant Sci. *16*, 579-581.

938 Aroca, A., Benito, J.M., Gotor, C., and Romero, L.C. (2017a). Persulfidation proteome
939 reveals the regulation of protein function by hydrogen sulfide in diverse biological
940 processes in Arabidopsis. J. Exp. Bot. *68*, 4915-4927.

941 Aroca A, Schneider M, Scheibe R, Gotor C, Romero LC. (2017b). Hydrogen sulfide
942 regulates the cytosolic/nuclear partitioning of glyceraldehyde-3-phosphate
943 dehydrogenase by enhancing its nuclear localization. Plant and Cell Physiology *58*,
944 983-992.

945 Aroca, A., Gotor, C., Romero, L.C. (2018) Hydrogen sulfide signaling in plants: emerging
946 roles of protein persulfidation. Front. Plant Sci. https://doi.org/10.3389/fpls.2018.01369.

947 Aroca, A., Serna, A., Gotor, C., and Romero, L.C. (2015). S-sulfhydration: a cysteine
948 posttranslational modification in plant systems. Plant Physiol. *168*, 334-342.

949 Batool, S., Uslu, V., Rajab, H., Ahmad, N., Waadt, R., Geiger, D., Malagoli, M., Xiang, C.,
950 Hedrich, R., Rennenberg, H., Herschbach, C., Hell, R., and Wirtz, M. (2018). Sulfate is
951 incorporated into cysteine to trigger ABA produciton and stomatal closure. Plant Cell *30*,
952 2973-2987.

953 Bauer, H., Ache, P., Lautner, S., Fromm, J., Hartung, W., Al-Rasheid, K., Sonnewald, S.,
954 Sonnewald, U., Kneitz, S., Lachmann, N., Mendel, R., Bittner, F., Hetherington, A., and
955 Hedrich, R. (2013). The stomatal response to reduced relative humidity requires guard
956 cell-autonomous ABA synthesis. Curr. Biol. *23*, 53-57.

957 Bernula, P., Crocco, C.D., Arongaus, A.B., Ulm, R., Nagy, F., and Viczián, A. (2017).
958 Expression of the UVB8 photoreceptor in different tissues reveals tissue-autonomous
959 features of UV-B signalling. Plant Cell Environ. *40*, 1104-1114.

960 Blatt, M. (2010). Cellular signaling and volume control in stomatal movements in plants.
961 Annu. Rev. Cell Dev.Biol. *16*. 221-241.

962 Bogdandi, V., T. Ida, T. R. Sutton, C. Bianco, T. Ditroi, G. Koster, H. A. Henthorn, M.
963 Minnion, J. P. Toscano, A. van der Vliet, M. D. Pluth, M. Feelisch, J. M. Fukuto, T. Akaike
964 and P. Nagy (2019). Speciation of reactive sulfur species and their reactions with
965 alkylating agents: do we have any clue about what is present inside the cell? Br J
966 Pharmacol. *176,* 646-670.

967 Boursiac, Y., Léran, S., Corratgéfaillie, C., Gojon, A., Krouk, G., and Lacombe, B. (2013).
968 ABA transport and transporters. Trends Plant Sci. *18*, 325-333.

969 Bright, J., Desikan, R., Hancock, J.T., Weir, I.S., and Neill, S.J. (2010). ABA-induced no
970 generation and stomatal closure in Arabidopsis are dependent on H_2O_2 synthesis. Plant J.
971 *45*, 113-122.

972 Cao, M.J., Wang, Z., Zhao, Q., Mao, J.L., Speiser, A., Wirtz, M., Hell, R., Zhu, J., and
973 Xiang, C. (2014). Sulfate availability affects ABA levels and germination response to ABA
974 and salt stress in Arabidopsis thaliana. Plant J. *77*, 604-615.

975 Chater, C., Peng, K., Movahedi, M., Dunn, J.A., Walker, H.J., and Liang, Y.K. (2015).
976 Elevated CO_2-induced responses in stomata require ABA and ABA signaling. Curr. Biol.
977 *25*, 2709-2716.

978 Chen, D., Cao, Y., Li, H., Kim, D., Ahsan, N., Thelen, J., and Stacey, G. (2017).
979 Extracellular ATP elicits DORN1-mediated RBOHD phosphorylation to regulate stomatal
980 aperture. Nat. Comm. 8, 2265-2677.

981 Chi, H., C. Liu, H. Yang, W. F. Zeng, L. Wu, W. J. Zhou, R. M. Wang, X. N. Niu, Y. H. Ding,
982 Y. Zhang, Z. W. Wang, Z. L. Chen, R. X. Sun, T. Liu, G. M. Tan, M. Q. Dong, P. Xu, P. H.

983 Zhang and S. M. He (2018). Comprehensive identification of peptides in tandem mass
984 spectra using an efficient open search engine. Nat Biotechnol. 36, 1059-1061.

985 Christmann, A., Weiler, E.W., Steudle, E., and Grill, E. (2007). A hydraulic signal in
986 root-to-shoot signalling of water shortage. Plant J. *52*, 167-174.

987 Corpas, F.J., González-Gordo, S., Cañas, A., and Palma, J.M. (2019). Nitric oxide (NO)
988 and hydrogen sulfide (H_2S) in plants: Which is first? J. Exp. Bot.
989 https://doi.org/10.1093/jxb/erz031.

990 Desikan, R., Cheung, M.K., Bright, J., Henson, D., Hancock, J.T., and Neill, S.J. (2004).
991 ABA, hydrogen peroxide and nitric oxide signalling in stomatal guard cells. J. Exp. Bot. *55,*
992 205-212.

993 Du, X.Z, Jin, Z.P., Zhang, L.P., Liu, X., Yang, G.D., and Pei, Y.X. (2019). H_2S is involved in
994 ABA-mediated stomatal movement through MPK4 to alleviate drought stress in
995 Arabidopsis thaliana. Plant Soil. *435*, 295-307.

996 Filipovic, M.R., and Jovanović, V.M. (2017). More than just an intermediate: hydrogen
997 sulfide signalling in plants. J. Exp. Bot. *68*, 4733-4736.

998 Filipovic, M.R., Zivanovic, J., Alvarez, B., and Banerjee, R. (2018). Chemical biology of
999 H_2S signaling through persulfidation. Chem. Rev. *118*, 1253-1337.

1000 Fu, L., K. Liu, J. He, C. Tian, X. Yu and J. Yang (2019). Direct Proteomic Mapping of
1001 Cysteine Persulfidation. Antioxid Redox Signal. Doi:10.1089/ars.2019.7777

1002 Garcia-Mata, C., and Lamattina, L. (2010). Hydrogen sulphide, a novel gasotransmitter
1003 involved in guard cell signalling. New Phytol. *188*, 977-984.

1004 Gilroy, S., Suzuki, N., Miller, G., Choi, W.G., Toyota, M., Devireddy, A.R., and Mitter, R.
1005 (2014) A tidal wave of signals: calcium and ROS at the forefront of rapid systemic
1006 signaling. Trends in Plant Sci. *19,* 623-630.

1007 Gotor, C., Garcia, I., Aroca, A., Laureano-Marin, A.M., Arenas-Alfonseca, L.,
1008 Jurado-Flores, A., Moreno, I., and Romero, L.C. (2019) Signaling by hydrogen sulfide and

cyanide through posttranslational modification. J Exp Bot. *70*, 4251-4265.

Guo, H.M., Xiao, T.Y., Zhou, H., Xie, Y.J., and Shen, W.B. (2016). Hydrogen Sulfide, a versatile regulator of environmental stress in Plants. Acta. Physiol. Plant *38*, 1-13.

Guo, H.M., Zhou, H., Zhang, J., Guan, W.X., Xu, S., Shen, W.B., Xu, G.H., Xie, Y.J., and Foyer, C.H. (2017). L-cysteine desulfhydrase-related H_2S production is involved in OsSE5-promoted ammonium tolerance in roots of *Oryza sativa*. Plant Cell & Environ, 2017, 40: 1777-1790

Hancock, J. (2019). Considerations of the importance of redox state for reactive nitrogen species action. J Exp. Bot. https://doi.org/10.1093/jxb/erz067.

Hauser, F., Li, Z., Waadt, R., and Schroeder, J.I. (2017). Snapshot: Abscisic Acid signaling. Cell *171*, 1708-1708.

Honda, K., Yamada, N., Yoshida, R., Ihara, H., Sawa, T., and Akaike, T. (2015). 8-mercapto-cyclic GMP mediates hydrogen sulfide-induced stomatal closure in Arabidopsis. Plant Cell Physiol. *56*, 1481-1489.

Huang, J., P. Willems, B. Wei, C. Tian, R. B. Ferreira, N. Bodra, S. A. Martinez Gache, K. Wahni, K. Liu, D. Vertommen, K. Gevaert, K. S. Carroll, M. Van Montagu, J. Yang, F. Van Breusegem and J. Messens (2019). Mining for protein S-sulfenylation in Arabidopsis uncovers redox-sensitive sites. Proc Natl Acad Sci U S A 116: 21256-21261.

Jin, Z., Xue, S., Luo, Y., Tian, B., Fang, H., Li, H., and Pei, Y. (2013). Hydrogen sulfide interacting with abscisic acid in stomatal regulation responses to drought stress in Arabidopsis. Plant Physiol. Biochem. *62*, 41-46.

Kim, T.H., Böhmer, M., Hu, H.H., Nishimurab, N., and Schroeder, J. (2010). Guard cell signal transduction network: advances in understanding abscisic acid, CO_2, and Ca^{2+} signaling. Annu. Rev. Plant Biol. *61*, 561-591.

Kirchenbauer, D., Viczian, A., Adam, E., Hegedus, Z., Klose, C., Leppert, M., and Nagy, F. (2016). Characterization of photomorphogenic responses and signaling cascades controlled by phytochrome-A expressed in different tissues. New Phytol. *211*, 584-598.

Kuromori, T., Sugimoto, E., Shinozaki, K. (2014) Intertissue signal transfer of abscisic acid from vascular cells to guard cells. Plant Physiol. *164*, 1587-1592.

Kwak, J.M., Mori, I.C., Pei, Z.M., Leonhardt, N., Torres, M.A., Dangl, J.L., Bloom, R.E., Bodde, S., Jones, J.D.G., and Schroeder J.I. (2003). NADPH oxidase AtrbohD and AtrbohF genes function in ROS-dependent ABA signaling in Arabidopsis. Embo J. *22*, 2623-2633.

Lai, D.W., Mao, Y., Zhou, H., Li, F., Wu, M.Z., Zhang, J., He, Z.Y., Cui, W.T., and Xie, Y.J. (2014) Endogenous hydrogen sulfide enhances salt tolerance by coupling the reestablishment of redox homeostasis and preventing salt-induced K^+-loss in seedlings of *Medicago sativa*. Plant Sci, *205*, 117-129.

Laureano-Marín, A.M., García, I., Romero, L.C., Gotor, C. (2014). Assessing the transcriptional regulation of L-CYSTEINE DESULFHYDRASE 1 in Arabidopsis thaliana. Front Plant Sci 5:683.

Li, J., Chen, S., Wang, X., Shi, C., Liu, H., Yang, J., Shi, W., Guo, J., and Jia, H. (2018). Hydrogen sulfide disturbs actin polymerization via S-sulfhydration resulting in stunted root hair growth. Plant Physiol. *178*, 936-949.

Ma, D., Ding, H., Wang, C., Qin, H., Han, Q., Hou, J., Lu, H., Xie, Y., and Guo, T. (2016). Alleviation of drought stress by hydrogen sulfide is partially related to the abscisic acid signaling pathway in wheat. PLoS One *9*, e0163082.

Magnani, F., Nenci, S., Millana, F.E., Ceccon, M., Romero, E., and Fraaije, M.W. (2017). Crystal structures and atomic model of NADPH oxidase. Proc. Natl. Acad. Sci. USA *114*, 6764-6769.

Marino, D., Dunand, C., Puppo, A., and Pauly, N. (2012). A burst of plant NADPH oxidases. Trends Plant Sci. *17*, 9-15.

Miller, G., Schlauch, K., Tam, R., Cortes, D., Torres, M.A., Shulaev, V., and Mittler, D.R. (2009). The plant NADPH oxidase RBOHD mediates rapid systemic signaling in response to diverse stimuli. Sci. Signal. *2*, ra45.

Mittler, R., Vanderauwera, S., Suzuki, N., Miller, G., Tognetti, V.B., Vandepoele, K., Gollery, M., Shulaev, V., Van Breusegem, F. (2011). ROS signaling: the new wave? Trends in Plant Sci. *16*, 300-309.

Nambara, E., and Marion-Poll, A. (2005). Abscisic acid biosynthesis and catabolism. Annu. Rev. Plant Biol. *56*,165-85.

Nühse, T.S., Bottrill, A.R., Jones, A.M.E., and Peck, S.C. (2007). Quantitative phosphoproteomic analysis of plasma membrane proteins reveals regulatory mechanisms of plant innate immune responses. Plant J. *51*, 931-947.

Ogasawara, Y., Kaya, H., Hiraoka, G., Yumoto, F., Kimura, S., Kadota, Y., Hishinuma, H., Senzaki, E., Yamagoe, S., Nagata, K., Nara, M., Suzuki, K., Tanokura, M., Kuchitsu, K. (2008). Synergistic activation of the Arabidopsis NADPH oxidase AtrbohD by Ca^{2+} and phosphorylation. J. Biol. Chem. *283*, 8885–8892.

Palde, P.B., and Carroll, K.S. (2015). A universal entropy-driven mechanism for thioredoxin-target recognition. Proc Natl Acad Sci U S A *112,* 7960-7965.

Papanatsiou, M., Scuffi, D., Blatt, M.R., and García-Mata, C. (2015). Hydrogen sulfide regulates inward-rectifying k^+ channels in conjunction with stomatal closure. Plant Physiol. *168*, 29-35.

Paul, B.D., and Snyder, S.H. (2012). H_2S signalling through protein sulfhydration and beyond. Nat. Rev. Mol. Cell Biol. *13,* 499-507.

Scuffi, D., Alvarez, C., Laspina, N., Gotor, C., Lamattina, L., and Garcia-Mata, C. (2014). Hydrogen sulfide generated by L-cysteine desulfhydrase acts upstream of nitric oxide to modulate abscisic acid-dependent stomatal clsoure. Plant Physiol. *166*, 2065-2076.

Scuffi, D., Nietzel, T., Fino, L.M.D., Meyer, A.J., Lamattina, L., Schwarzländer, M., Laxalt, A.M., and García-Mata, C. (2018). Hydrogen sulfide increases production of NADPH oxidase-dependent hydrogen peroxide and phospholipase D-derived phosphatidic acid in guard cell signaling. Plant Physiol. *176*, 2532-2542.

Sen, N., Paul, B.D., Gadalla, M.M., Mustafa, A.K., Sen, T., and Xu, R. (2012). Hydrogen

sulfide-linked sulfhydration of NF-κB mediates its antiapoptotic actions. Mol. Cell *45*, 13-24.

Sirichandra, C., Gu, D., Hu, H.C., Davanture, M., Lee, S., Djaoui, M., Valot, B., Zivy, M., Leung, J., Merlot, S., and Kwak, J. (2009). Phosphorylation of the Arabidopsis AtrbohF NADPH oxidase by OST1 protein kinase. FEBS Lett. *583*, 2982-2986.

Shevchenko, A., H. Tomas, J. Havlis, J. V. Olsen and M. Mann (2006). In-gel digestion for mass spectrometric characterization of proteins and proteomes. Nat Protoc 1: 2856-2860.

Shen. J., Su. Y., Zhou. C., Zhang. F., Zhou. H., Liu. X., Wu. D.L., Yin. X.C., Xie. Y.J., Yuan. X.X. (2019) A putative rice L-cysteine desulfhydrase encodes a true L-cysteine synthase that regulates plant cadmium tolerance. Plant Growth Regul, doi: 10.1007/s10725-019-00528-9.

Smirnoff, N., and Arnaud, D. (2019). Hydrogen peroxide metabolism and functions in plants. New Phytol. *221*, 1197-1214.

Song, Y., Miao, Y., and Song, C.P. (2014). Behind the scenes: the roles of reactive oxygen species in guard cells. New Phytol. *201*, 1121-1140.

Suzuki, N., Miller, G., Morales, J., Shulaev, V., Torres, M.A., and Mittler, R. (2011). Respiratory burst oxidases: the engines of ROS signaling. Curr. Opin. Plant Biol. *14*, 691-699.

Tan, B.C., Joseph, L.M., Deng, W.T., Liu, L.J., Li, Q.B., Cline, K., McCarty, D.R. (2003) Molecular characterization of the Arabidopsis nine-cis expoxycarotenoid dioxygenase gene family. Plant J. *35*, 44-56.

Vandiver, M., Paul, B., Xu, R., Karuppagounder, K., Rao, F., Snowman, A., Ko, H., Lee, Y., Dawson, V., Dawson, T., Sen, N., and Snyder, S. (2013) Sulfhydration mediates neuroprotective actions of parkin. Nat Comm. *4,* 1626

Wang, P., and Song, C.P. (2008). Guard-cell signalling for hydrogen peroxide and abscisic acid. New Phytol. *178*, 703-718.

Xie, Y.J., Zhang, C., Lai, D.W., Sun, Y., Samma, M.K., Zhang, J., and Shen, W.B. (2014) Hydrogen sulfide delays GA-triggered programmed cell death in wheat aleurone layers by the modulation of glutathione homeostasis and heme oxygenase-1 expression. J Plant Physiol *171*, 53-62.

Xie, Y.J., Lai, D.W., Mao, Y., Zhang, W., Shen, W.B., and Guan, R.Z. (2013) Molecular cloning, characterization and expression analysis of a novel gene encoding L-cysteine desulfhydrase from *Brassica napus*. Mol Biotechnol, *54,* 737-746.

Yun, B.W., Feechan, A., Yin, M.H., Saidi, N.B.B., Le, B.T., Yu, M., Moore, J.W., Kang, J.G., Kwon, E., Spoel, S.H., Pallas, J.A., and Loake, G.J. (2011). S-nitrosylation of NADPH oxidase regulates cell death in plant immunity. Nature *478*, 264-268.

Zhang, J., Zhou, M.J., Ge, Z.L., Shen, J., Zhou, C., Gotor, C., Romero, L.C., Duan, X.L., Liu, X., Wu, D.L., Yin, X.C., and Xie, Y.J. (2019) ABA-triggered guard cell L-cysteine desulfhydrase function and in situ H_2S production contributes to heme oxygenase-modulated stomatal closure. Plant Cell & Environ, doi: 10.1111/pce.13685

Zhu J. (2016). Abiotic stress signaling and responses in plants. Cell *167*, 313-324.

Figure legends

Figure 1. Regulation of DES1 Protein by Persulfidation

(A) Sulfurating molecule-induced persulfidation and activity of the DES1 recombinant protein. Purified DES1 recombinant protein was treated with sulfurating molecule NaHS (1 mM) for 1 hr, dialyzed and then divided into two aliquots, one was used to measure the DES enzyme activity and the other was then subjected to a tag-switch assay for the analysis of the protein persulfidation (DES1-SSH). Treatment with DTT (1 mM) is shown as negative control. The DES activity data represent mean ± SD (n = 3) from three biological replicates. Different letters were different significantly at $P < 0.05$ according to one-way ANOVA (post-hoc Tukey's HSD test).

(B) Analysis of persulfidation of DES1-GFP in guard cells. Total proteins were extracted from *pMYB60:DES1-GFP des1* transgenic plants after exposure to different concentrations of NaHS or DTT (1 mM) for 1 hr, and subjected to the tag-switch assay.

(C) ABA-induced persulfidation of DES1 in guard cells. Total proteins extracted from *pMYB60:DES1-GFP des1* transgenic plants were subjected to the tag-switch assay after exposure to ABA treatment (10 μM) for the indicated times.

For *in vitro* assay, the persulfidated recombinant protein was detected by an anti-biotin antibody after tag-switch labeling. Con, control. CBB, Coomassie Brilliant Blue protein stain. IB, Immunoblotting. For *in vivo* assay, 4-week-old plants grown in the soil were treated and harvested at the indicated times. The persulfidated DES1-GFP protein in guard cells was detected by an anti-GFP antibody after tag-switch labeling and streaptavidin purification. The bottom panels show that the total DES1-GFP used for the tag-switch assay. The numbers above the bottom panels indicate the relative abundance of the corresponding persulfidated protein compared with that of the control sample (1.00). Signals from two independent experiments were quantified.

Figure 2. Regulation of DES1 Protein by Persulfide-Oxidation

(A and C) H_2O_2-triggered oxidation and down-regulation of activity of the persulfidated DES1-His recombinant protein *in vitro*. Persulfidated DES1-His recombinant protein was treated with H_2O_2 at wide range of concentrations for 1 hr (A) or increasing time period (10 μM H_2O_2 for C), and then divided into two aliquots, one was used to measure the DES enzyme activity and the other was subjected to a tag-switch assay for the analysis of the level of persulfidation of DES1 (DES1-SSH). The DES1 activity data represent mean ± SD (n = 3) from three biological replicates. Different letters were different significantly at $P < 0.05$ according to one-way ANOVA (post-hoc Tukey's HSD test).

(B) H_2O_2-triggered oxidation of persulfidated DES1 in guard cells. Total proteins extracted from *pMYB60:DES1-GFP des1* transgenic plant were subjected to the tag-switch assay after exposure to H_2O_2 at different concentrations for 1 hr. Two images of the same blot with different time of exposure are shown.

(D) Enhancement of ABA-induced DES1 persulfidation by DPI in guard cells. Total proteins extracted from *pMYB60:DES1-GFP des1* transgenic plants were subjected to the tag-switch assay after exposure to ABA at 10 μM for 30 min, with or without pretreatment of DPI at 10 μM for 2 hr.

(E) ABA- and H_2O_2-regulated persulfidation of DES1 in guard cells. Total proteins extracted from *pMYB60:DES1-GFP des1* and *pMYB60:DES1-GFP des1 rbohD* transgenic plants were subjected to the tag-switch assay after exposure to ABA treatment at 10 μM for 30 min.

(F and G) Reversible persulfidation and persulfide-oxidation of DES1-His recombinant protein. Purified DES1 recombinant protein was NaHS pretreated at 10 μM for 1 h, followed by dialysis and then treated with H_2O_2 at 10 uM for the indicated times (F), or H_2O_2 pretreated at 10 uM for 1hr, followed by dialysis and treated with NaHS at 10 μM for the indicated times (G), and then subjected to a tag-switch assay for the analysis of the persulfidation level (DES1-SSH).

For *in vitro* assay, the persulfidated recombinant protein was detected by an anti-biotin antibody after the tag-switch labeling. CBB, Coomassie Brilliant Blue protein stain. IB, Immunoblotting. For *in vivo* assay, 4-week-old plants grown in the soil were treated and harvested at the indicated times. The persulfidated DES1-GFP protein in guard cells was detected by an anti-GFP antibody after tag-switch labeling and streptavidin purification. The bottom panels show that the total DES1-GFP used for the tag-switch assay as loading control. The numbers above the bottom panel indicate the relative abundance of the corresponding persulfidated protein compared with that of the control sample (1.00). Signals from two independent experiments were quantified.

Figure 3 Persulfidation of DES1 on Cys44 and Cys205 Regulates ABA-Induced Stomatal Closure

(A and B) Fully annotated MS/MS spectra of IAM-derivatized DES1 peptides containing persulfided cysteines. Purified recombinant DES1 protein was treated with NaHS (1 mM for 1 hr), alkylated with iodoacetamide (IAM), and analyzed by LC-MS/MS. The localization of IAM-derivatized persulfides was unequivocally annotated according to the modification-specific b- or y-ions .

(C and D) *In vitro* persulfidation analysis of DES1 and mutant recombinant proteins by the tag-switch method. The persulfidated protein was detected by an anti-biotin antibody.

(E) *In vivo* persulfidation analysis of the mutated versions of DES1 protein. Total proteins from Arabidopsis protoplasts transiently expressed DES1 and its mutant derivatives fused to GFP were subjected to the tag-switch assay for the analysis of the level of persulfidation of different versions of DES1(DES1-SSH). The bottom panel shows the total DES1-GFP used for the tag-switch assay as loading control.

(F) Effect of ABA and NaHS on the persulfidation level of DES1 *in vivo*. Total proteins from Arabiodopsis protoplasts transiently expressed unmutated DES1 fused to GFP were treated with or without ABA (10 μM for 30 min) or NaHS (1

mM for 1 hr) before subjected to the tag-switch assay for the analysis of the level of persulfidation (DES1-SSH). The bottom panel shows the total DES1-GFP used for the tag-switch assay as loading control.

(G) DES enzyme activity of different versions of the DES1-His recombinant proteins in the presence or absence of NaHS or H_2O_2. Recombinant proteins were pretreated with either NaHS (10 μM) or H_2O_2 (10 μM) for 1hr. Con means untreated conditions. The data represent mean ± SD (n = 3) from three biological replicates. Bars denoted by the different letters were different significantly at $P < 0.05$ according to one-way ANOVA (post-hoc Tukey's HSD test).

(H) Reversibility of the enzyme activity of DES1-His recombinant protein (wildype) and its mutant derivative Cys44/205Ala. Recombinant proteins were pretreated with either NaHS (10 μM) or DTT (1 mM) for 1hr, followed by dialysis and then treated with the H_2O_2 (10 μM) at the indicated times. The data represent mean ± SD (n = 3) from three biological replicates. Different letters were different significantly at $P < 0.05$ according to one-way ANOVA (post-hoc Tukey's HSD test).

(I and J) Effects of ABA and NaHS on the guard cell H_2S production and stomatal closure of wild type, the *des1*, and the *des1* with different mutated varieties. H_2S production was monitored using the fluorescent dye 7-Azido-4-Methylcoumarin (AzMC). Epidermal strips of each line were pre-incubated for 3 hr in opening buffer (10 mM MES, pH 6.15, and 10 mM KCl) under light (120 μE $m^{-2}s^{-1}$) and loaded with AzMC (15 μM) for 40 min before washing in MES buffer three times for 15 min each. Subsequently, samples were treated for 30 min with ABA (10 μM), NaHS (100 μM) or H_2O_2 (10 μM), respectively. For (G), the value 100% corresponds to the fluorescence of wild type in control conditions. R.U., relative units. The corresponding stomatal aperture sizes were also measured. The data represent mean ± SD from three biological replicates ($n \geq 90$ in each replicate). Bars denoted by the different

letters were different significantly at $P < 0.05$ according to two-way ANOVA (post-hoc Tukey's HSD test).

(K) Stomatal closure and H_2S production rate of different plant lines under ABA treatment for the indicated times. Treatment and measurement details are described in Figure. 3I and J. The data represent mean ± SD from three biological replicates ($n \geq 90$ in each replicate). Asterisks represent significant differences between *pMYB60:DES1 des1* and *pMYB60:DES1Cys44/205Ala des1* according to Student's t-test (*P < 0.05, **P < 0.01, ***P < 0.001).

4-week-old plants grown in the soil were treated and harvested at the indicated times. For the immunoblot, the numbers upon the bottom panels indicate the relative abundance of the corresponding persulfidated protein compared with that of the control sample (1.00). Signals from two independent experiments were quantified. CBB, Coomassie Brilliant Blue protein stain. IB, Immunoblotting. Wild type represents the unmutated version of DES1 protein.

Figure 4. H_2S Requires RBOHD Activity for the Induction of Stomatal Closure

(A) ROS production in guard cells and stomatal responses of wild type, *rbohD*, and *rbohD* rescued lines. RBOHD was rescued by expressing RBOHD under the control of tissue-specific promoters, in which RBOHD was expressed in guard cells (*pMYB60: RBOHD*), epidermal (*pML1: RBOHD*), or mesophyll cells (*pCAB3: RBOHD*) individually. ROS production was monitored using florescent dye H_2DCFDA (upper panel). Epidermal strips of each line were pre-incubated for 3 hr in opening buffer (10 mM MES, pH 6.15, and 10 mM KCl) under light (120 µE $m^{-2}s^{-1}$) and loaded with H_2DCFDA (15 µM) for 15 min before washing in MES buffer three times for 15 min each. Subsequently, samples were treated for 1 hr with ABA (10 µM), NaHS (100 µM) or H_2O_2 (10 µM), respectively. The value 100% corresponds to the fluorescence of wild type (Col-0) in control conditions. R.U., relative units. The corresponding stomatal aperture sizes were also measured (lower panel). The data represent

mean ± SD from three biological replicates (n ≥ 90 in each replicate). Bars denoted by the different letters were different significantly at P < 0.05 according to two-way ANOVA (post-hoc Tukey's HSD test).

(B) ABA- and NaHS-induced net H_2O_2 influxes in guard cells of *rbohD* and *pCAB3:RBOHD rbohD* plants. Leaves from 4-week-old plant were preincubated for 3 hr in opening buffer (10 mM MES, pH 6.15, and 10 mM KCl) under light (120 μE $m^{-2}s^{-1}$) and washed in MES buffer three times for 15 min each. The net H_2O_2 influxes were observed after ABA (10 μM) or NaHS (100 μM) treatment during the indicated times (n = 6)

(C) ROS production in guard cells and stomatal responses of wild type, *des1*, *des1/rbohD*, and *des1/rbohD* rescued lines. Treatment and measurement details are shown in Figure. 4A.

(D-F) Effects of sulfurating molecules on NADPH oxidase activity of wild type, *des1*, *rbohD*, and *rbohD* rescued line. For NADPH oxidase activity assay, the crude membrane extracts from each line (4-week-old) were extracted and treated with NaHS or Na_2S at indicated concentrations (0 - 1 mM; for F, NaHS at 100 μM) for 30 mins. NADPH oxidase activity was determined after dialysis. The data represent mean ± SD (n = 3) from three biological replicates. Different letters were different significantly at P < 0.05 according to two-way ANOVA (post-hoc Tukey's HSD test).

Figure 5. ABA-Induced Persulfidation of RBOHD at Cys825 and Cys890

(A) The C terminus of RBOHD is persulfidated in the presence or absence of two sulfurating molecules. RBOHD-C terminal recombinant protein was treated with NaHS or Na_2S at 1 mM for 1 hr before to be subjected to tag switch assay.

(B) Analysis of persulfidation of RBOHD-C terminal *in vivo*. Total proteins from Arabidopsis wild type protoplast transformed with *35S:RBOHD-C-GFP* were extracted and exposed to NaHS for 1 hr at the indicated concentrations, followed by the tag-switch assay.

(C) The N terminus of RBOHD is not persulfidated. RBOHD-N terminal recombinant protein was treated with NaHS 1 mM for 1 hr before to be subjected to tag switch assay.

(D) ABA-induced persulfidation of RBOHD-C terminal *in vivo*. Total proteins from Arabidopsis wild type (Col-0) and *des1* mutant protoplasts transformed with *35S:RBOHD-C-GFP* were extracted and treated with or without ABA at 10 μM for 30 min, followed by the subject to the tag-switch assay.

(E and F) H_2O_2-triggered persulfide-oxidation of the RBOHD-C terminal recombinant protein *in vitro* (E) or RBOHD-C-GFP protein *in vivo* (F). Samples were treated with H_2O_2 at indicated concentrations for 1 hr before to be subjected to the tag-switch assay.

(G) Enhancement of ABA-induced RBOHD-C-GFP persulfidation by DPI. Total proteins from Arabidopsis protoplast transformed with *35S:RBOHD-C-GFP* were subjected to the tag-switch assay after exposure to ABA at 10 μM for 30 min, with or without pretreatment of DPI at 10 μM for 2 hr.

(H-J) Persulfidation analysis of the C terminus of wild type and mutant RBOHD derivatives *in vitro* (H) and *in vivo* (I and J).

For *in vitro* assay, the persulfidated recombinant proteins were detected by an anti-biotin antibody after the tag-switch labeling. Proteins were detected by immunoblotting using an anti-his antibody served as a loading control. Con, control. CBB, Coomassie Brilliant Blue protein stain. For *in vivo* assay, total proteins from Arabidopsis protoplasts transiently expressed the RBOHD C terminus and its mutant derivatives fused to GFP were treated with or without ABA (10 μM for 30 min) or NaHS (1 mM for 1 hr) before to be subjected to the tag-switch assay and streptavidin purification. The persulfidated proteins were detected by an anti-GFP antibody. The bottom panels show the total GFP fused proteins used for the tag-switch assay as loading control. Wild type represents the unmutated version of RBOHD-C protein and Con means untreated conditions. The numbers above the bottom panels indicate the relative abundance of the corresponding persulfidated protein compared with

that of the control sample (1.00). Signals from two independent experiments were quantified.

Figure 6. DES1-Triggered Persulfidation of RBOHD at C825 and C890 is Involved in ABA-Induced ROS Activation and Stomatal Closure.

(A) Effects of NaHS or DTT on the activity of NADPH oxidase of mutant *rbohD* plants expressing either a wild type RBOHD or Cys825Ala, Cys890Ala and Cys825/890Ala mutant derivatives driven by its native promoter. Treatment and measurement details are represented in Figure. 4D-F.

(B and C) Effects of ABA or NaHS on ROS production and stomatal closure of wild type (Col-0), *rbohD*, *des1 rbohD*, and lines expressing either a wild type RBOHD or Cys825Ala, Cys890Ala and Cys825/890Ala mutant derivatives driven by its native promoter. Treatment and measurement details are shown in Figure. 4A.

Figure 7. Working Model Shown in This Study. While drought stress signal was sensed by the plant, ABA was synthesized and triggered rapid and strong expression of DES1 in guard cells by unknown mechanism. Inducible DES1 expression can persulfide many downstream signaling proteins, including itself on Cys44 and Cys205, and leading to the amplification of guard cell H_2S signals. The inducible DES1/H_2S also persulfidates NADPH oxidase RBOHD on Cys825 and Cys890 to facilitate the rapid induction of ROS burst, which in turn causes stomatal closure. When ROS accumulates to high levels, it further causes persulfide-oxidation of RBOHD and DES1 (-SSO_nH), leading to ABA de-sensitivity. The oxidized persulfide (-SSO_nH) may subsequently be reduced to thiol group (-SH) by thioredoxin, which formed a feed-back prevention of ABA signaling continuously activated in guard cells.

SUPPLEMENTAL INFORMATION

Supplemental Figure 1 Analysis of persulfidation of DES1-GFP *in vivo*. Total proteins were extracted from *pMYB60:DES1-GFP des1* transgenic plants. The persulfidated DES1-GFP protein was detected by an anti-GFP antibody after tag-switch labeling with or without cyano-biotin and streptavidin purification. The bottom panels show that the total DES1-GFP used for the tag-switch assay. The bars below indicate the relative abundance of the corresponding persulfidated protein compared with that of the control sample (1.0). Signals from two independent experiments were quantified.

Supplemental Figure 2 Relative expression of *DES1* in wild type (Col-0), *des1* and lines expressing either a wild type DES1 or Cys30Ala, Cys44Ala, Cys205Ala and Cys30/44/205Ala mutant derivatives driven by *MYB60* promoter. Complementation analyses were conducted using RT-qPCR. Total RNA was isolated from 7-day-old seedling leaves living on 1/2 MS medium. Corresponding expression levels are presented relative to that of *UBQ*, taking values for the control sample as 100%. Data are mean ± SD of three independent experiments with at least three biological replicates for each individual experiment. Bars denoted by the different letters were significantly different at $P < 0.05$ according to one-way ANOVA (post-hoc Tukey's HSD test).

Supplemental Figure 3. Detection of persulfidation of the DES1 protein *in vivo*. DES1-GFP total protein extracted from *pMYB60:DES1-GFP des1* transgenic plants. DES1-GFP protein was treated with the slow-release H_2S donor GYY4137 dichloromethane Complex (A) and JK-2 (B) for 1 h, and then subjected to a tag-switch assay for the analyses of the S-persulfidation level. The bars below indicate the relative abundance of the corresponding persulfidated protein compared with that of the control sample (1.0). Signals

from two independent experiments were quantified. Bars denoted by the different letters were different significantly at $P < 0.05$ according to one-way ANOVA (post-hoc Tukey's HSD test).

Supplemental Figure 4. Analysis of persulfidation of RBOHD-C terminal *in vivo*. Total proteins from Arabidopsis wild type protoplasts transformed with *35S:DES1-GFP* or *35S:GFP* were extracted and subjected to the tag-switch assay. Persulfidation level was detected by using anti-biotin antibody. GFP and DES1-GFP proteins were detected by immunoblotting using an anti-GFP antibody.

Supplemental Figure 5. Time-dependent persulfidation oxidation of DES1-His recombinant protein. The DES1 recombinant protein were treated with H_2O_2 (100 μM) and sampled at the indicated times, and subjected to the tag-switch assay. CBB, Coomassie Brilliant Blue protein stain. The bars below indicate the relative abundance of the corresponding persulfidated protein compared with that of the control sample (1.0). Bars denoted by the different letters were different significantly at $P < 0.05$ according to one-way ANOVA (post-hoc Tukey's HSD test).

Supplemental Figure 6. Persulfidation of DES1-His recombinant protein by H_2O_2 pretreatment. Purified DES1-His recombinant protein was treated with NaHS (1 mM) after pretreatment of H_2O_2 (10 μM) for 1 hr, and then subjected to a tag-switch assay for the analyses of the persulfidation (DES1-SSH). The bars below indicate the relative abundance of the corresponding persulfidated protein compared with that of the control sample (1.0). Bars denoted by the different letters were different significantly at $P < 0.05$ according to one-way ANOVA (post-hoc Tukey's HSD test).

Supplemental Figure 7. Amino acid sequence of DES1 protein. DES1 protein has 323 amino acids in total. The yellow markers indicate cysteines 30, 44 and 205.

Supplemental Figure 8. The persulfidation formation of DES1-His recombinant protein and its derivatives Cys44Ala, Cys205Ala, Cys44/205Ala, and Cys30/44/205Ala. Recombinant proteins were treated with NaHS or DTT (1 mM) individually, then subjected to a tag-switch assay for the analyses of the persulfidation (DES1-SSH). CBB, Coomassie Brilliant Blue protein stain. The bars below indicate the relative abundance of the corresponding persulfidated protein compared with that of the control sample (1.0). Bars denoted by the different letters were different significantly at $P < 0.05$ according to one-way ANOVA (post-hoc Tukey's HSD test).

Supplemental Figure 9. Representative images of ABA on the guard cell H_2S production of *des1* rescued lines shown in Figure 3G.

Supplemental Figure 10. The effects of NaHS on the guard cell H_2S production (A) and stomatal closure (B) of wild type, *des1*, and *des1* rescued lines. Samples were treated for NaHS (100 μM). Treatment and measurement details are shown in Figure. 3G-H.

Supplemental Figure 11 Relative expression of *RBOHD* in wild type (Col-0), *rbohD* and lines expressing *RBOHD* under the control of tissue-specific promoters, in which *RBOHD* was expressed in mesophyll cells (*pCAB3:RBOHD*), epidermal (*pML1:RBOHD*), or guard cells (*pMYB60:RBOHD*) individually. Complementation analyses were conducted by using RT-qPCR. Total RNA was isolated from 7-day-old seedling leaves living on 1/2 MS medium. Corresponding expression levels are presented relative to that of *UBQ*, taking values for the control sample as 100%. Data are

mean ± SD of three independent experiments with at least three biological replicates for each individual experiment. Bars denoted by the different letters were different significantly at $P < 0.05$ according to one-way ANOVA (post-hoc Tukey's HSD test).

Supplemental Figure 12. Representative images of guard cell ROS production for *rbohD* and its rescued lines shown in Figure 4A. Bar = 15 μm.

Supplemental Figure 13. Genotyping for the *des1 rbohD* mutant. Primers (Supplemental Data Set 1) used include LBb1.3 and dspm1 from the specific and transposon primers from each *des1* and *rbohD* gene: *des1*-LP, *des1*-RP, *rbohD*-LP and *rbohD*-RP (A). Insertions in *des1 rbohD* were identified through a PCR screen on genomic DNA extracted from pools of mutant plants containing LBb1.3 and dspm1 transposon insertions (B).

Supplemental Figure 14. Stomatal responses of wild type, *des1 rbohD*, and *des1 rbohD* rescued lines. RBOHD was rescued by expressing RBOHD under the control of tissue-specific promoters, in which RBOHD was expressed in guard cells (*pMYB60:RBOHD*), epidermal (*pML1: RBOHD*), or mesophyll cells (*pCAB3: RBOHD*) individually. Treatment and measurement details are shown in Figure. 3G-H and 4A.

Supplemental Figure 15 Subcellular Localization of RBOHD-C-GFP. Constructs carrying RBOHD-C-GFP and was introduced into Arabidopsis protoplasts, and the transfected protoplasts were observed after a 16-h incubation using a laser confocal microscope. The photographs were taken in the green channel (488 nm) for RBOHD-C-GFP, red channel (640 nm) for chloroplast auto-fluorescence. Scale bars: 10 μm.

Supplemental Figure 16 Detection for the persulfidation of the RBOHD-C

terminal *in vivo*. Arabidopsis wild type protoplasts transformed with *35S:RBOHD-C-GFP* were treated with the slow-release H_2S donor GYY4137 dichloromethane complex (A) and JK-2 (B) for 1 h, and then subjected to a tag-switch assay for the analyses of the S-persulfidation level. The bars below indicate the relative abundance of the corresponding persulfidated protein compared with that of the control sample (1.0). Signals from two independent experiments were quantified. Bars denoted by the different letters were different significantly at $P < 0.05$ according to one-way ANOVA (post-hoc Tukey's HSD test).

Supplemental Figure 17. A time-dependent decrease of persulfidation of RBOHD-C recombinant protein *in vitro*. The RBOHD-C recombinant protein were treated with H_2O_2 (10 μM). Samples were collected at the indicated times, and subjected to a tag-switch assay for the analyses of the persulfidation (RBOHD-C-SSH). Proteins were detected by immunoblotting using an anti-his antibody served as a loading control. The bars below indicate the relative abundance of the corresponding persulfidated protein compared with that of the control sample (1.0). Bars denoted by the different letters were different significantly at $P < 0.05$ according to one-way ANOVA (post-hoc Tukey's HSD test).

Supplemental Figure 18. Reversible persulfidation of RBOHD-C recombinant protein *in vitro*. Purified RBOHD-C recombinant protein was pre-treated with H_2O_2 at 10 μM (A) or 100 μM (B) for 1 h, followed by dialysis and treated by NaHS treatment at 10 μM, and then subjected to a tag-switch assay for the analyses of the persulfidation (RBOHD-C-SSH). Proteins were detected by immunoblotting using an anti-his antibody served as a loading control. The bars below indicate the relative abundance of the corresponding persulfidated protein compared with that of the control sample (1.0). Bars denoted by the different letters were different significantly at $P < 0.05$

according to one-way ANOVA (post-hoc Tukey's HSD test).

Supplemental Figure 19. Persulfidation of RBOHD-C recombinant protein and relative derivatives. The Cys825Ala and Cys890Ala derivatives were treated with two sulfurating molecules, NaHS (1 mM) and Na_2S (1 mM), separately for 1 h, and then subjected to a tag-switch assay for the analyses of the persulfidation (RBOHD-C-SSH). Proteins were detected by immunoblotting using an anti-his antibody served as a loading control. The bars below indicate the relative abundance of the corresponding persulfidated protein compared with that of the control sample (1.0). Bars denoted by the different letters were different significantly at $P < 0.05$ according to one-way ANOVA (post-hoc Tukey's HSD test).

Supplemental Figure 20. Persulfidation of the RBOHC-C recombinant proteins and related derivatives. wild type RBOHC-C, Cys809Ala, Cys874Ala and Cys809/874Ala recombinant proteins were subjected to a tag-switch assay for the analyses of the persulfidation. Reference proteins were detected by immunoblotting (IB) using an anti-his antibody. The bars below indicate the relative abundance of the corresponding persulfidated protein compared with that of the control sample (1.0). Bars denoted by the different letters were different significantly at $P < 0.05$ according to one-way ANOVA (post-hoc Tukey's HSD test).

Supplemental Figure 21. Relative expression of *RBOHD* in wild type (Col-0), *rbohD* and lines expressing either a wild type RBOHD or Cys825Ala, Cys890Ala and Cys825/890Ala mutant derivatives driven by its native promoter individually. Complementation analyses was conducted by using real-time RT-PCR. Total RNA was isolated from 7-day-old seedling leaves living on 1/2 MS medium. Corresponding expression levels are presented relative to that of *UBQ*, taking values for the control sample as 100%. Data are

mean ± SD of three independent experiments with at least three biological replicates for each individual experiment. Bars denoted by the different letters were different significantly at $P < 0.05$ according to one-way ANOVA (post-hoc Tukey's HSD test).

Supplemental Figure 22. Immunoblot membrane scans for this study.

Supplemental Data Set 1. Oligonucleotide primers used in this study.

Supplemental Data Set 2. Materials used in this study.

Supplemental Data Set 3. Detailed statistical analyses of the results in this study.

Figure 1

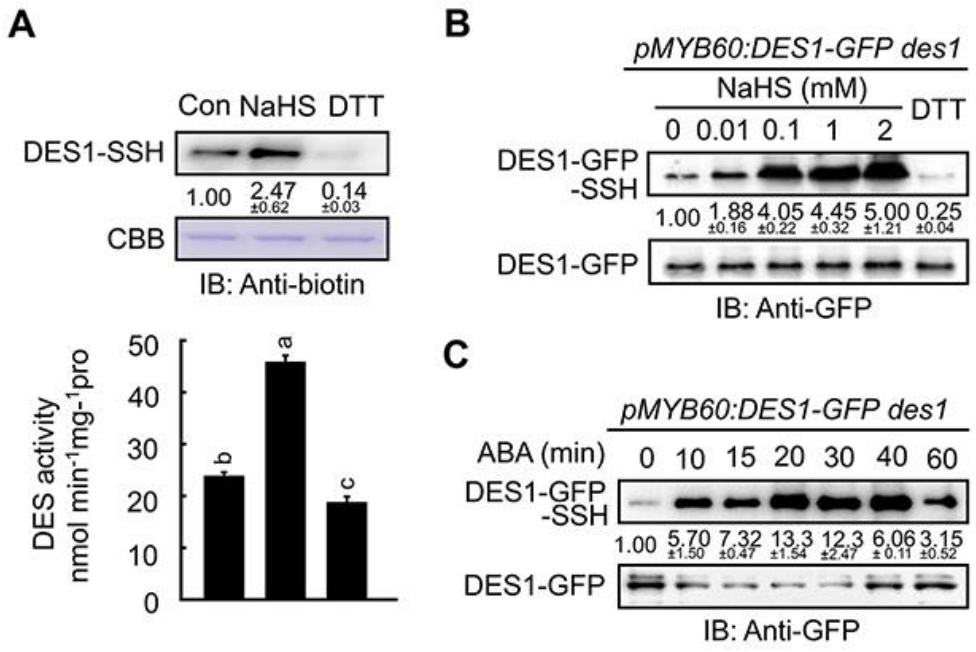

Figure 1. Regulation of DES1 Protein by Persulfidation

(A) Sulfurating molecule-induced persulfidation and activity of the DES1 recombinant protein. Purified DES1 recombinant protein was treated with sulfurating molecule NaHS (1 mM) for 1 hr, dialyzed and then divided into two aliquots, one was used to measure the DES enzyme activity and the other was then subjected to a tag-switch assay for the analysis of the protein persulfidation (DES1-SSH). Treatment with DTT (1 mM) is shown as negative control. The DES activity data represent mean ± SD (n = 3) from three biological replicates. Different letters were different significantly at $P < 0.05$ according to one-way ANOVA (post-hoc Tukey's HSD test).

(B) Analysis of persulfidation of DES1-GFP in guard cells. Total proteins were extracted from *pMYB60:DES1-GFP des1* transgenic plants after exposure to different concentrations of NaHS or DTT (1 mM) for 1 hr, and subjected to the tag-switch assay.

(C) ABA-induced persulfidation of DES1 in guard cells. Total proteins extracted from *pMYB60:DES1-GFP des1* transgenic plants were subjected to the tag-switch assay after exposure to ABA treatment (10 μM) for the indicated times.

For *in vitro* assay, the persulfidated recombinant protein was detected by an anti-biotin antibody after tag-switch labeling. Con, control. CBB, Coomassie Brilliant Blue protein stain. IB, Immunoblotting. For *in vivo* assay, 4-week-old plants grown in the soil were treated and harvested at the indicated times. The persulfidated DES1-GFP protein in guard cells was detected by an anti-GFP antibody after tag-switch labeling and streaptavidin purification. The bottom panels show that the total DES1-GFP used for the tag-switch assay. The numbers above the bottom panels indicate the relative abundance of the corresponding persulfidated protein compared with that of the control sample (1.00). Signals from two independent experiments were quantified.

Figure 2

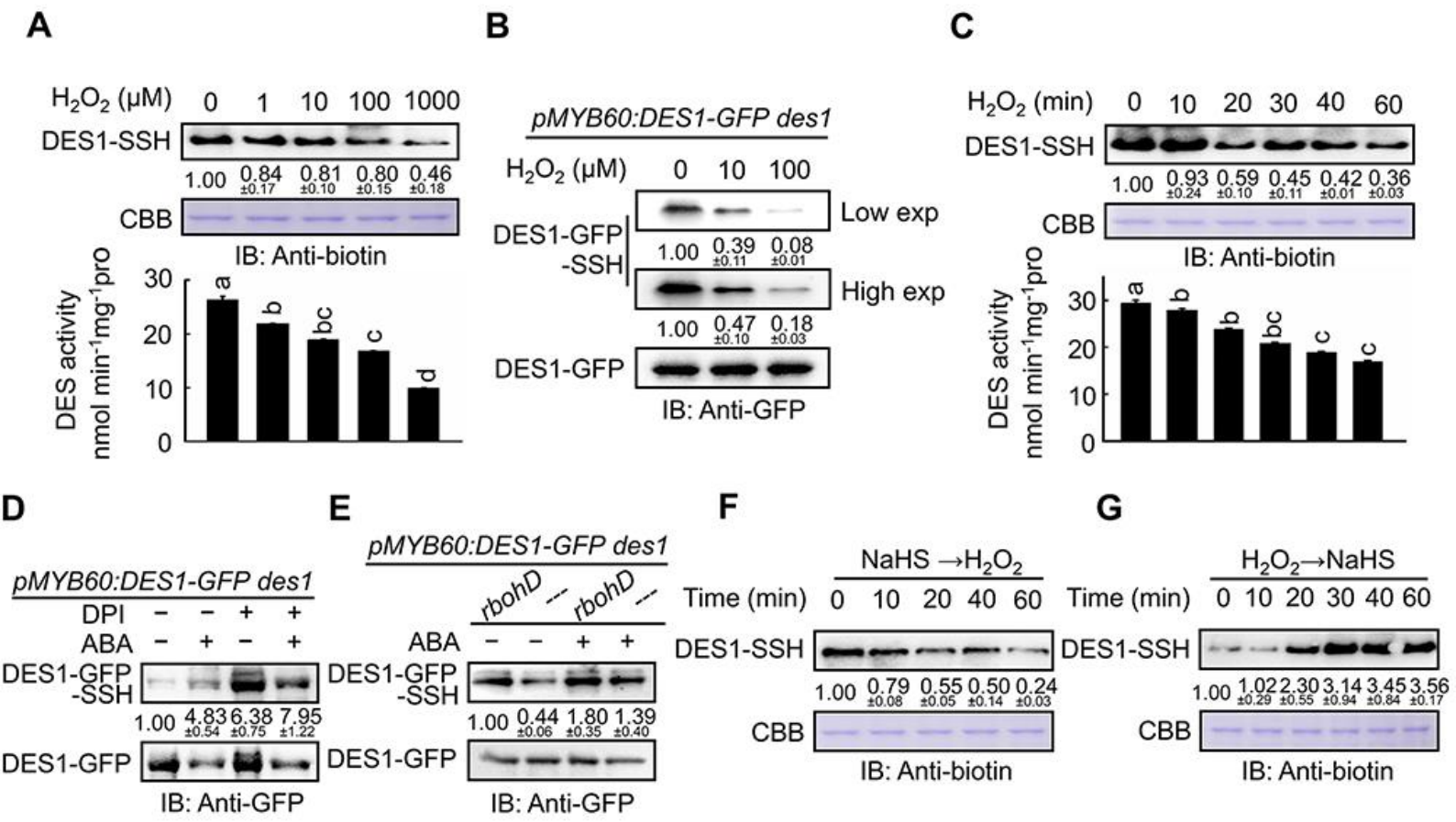

Figure 2. Regulation of DES1 Protein by Persulfide-Oxidation

(A and C) H_2O_2-triggered oxidation and down-regulation of activity of the persulfidated DES1-His recombinant protein *in vitro*. Persulfidated DES1-His recombinant protein was treated with H_2O_2 at wide range of concentrations for 1 hr (A) or increasing time period (10 μM H_2O_2 for C), and then divided into two aliquots, one was used to measure the DES enzyme activity and the other was subjected to a tag-switch assay for the analysis of the level of persulfidation of DES1 (DES1-SSH). The DES1 activity data represent mean ± SD (n = 3) from three biological replicates. Different letters were different significantly at $P < 0.05$ according to one-way ANOVA (post-hoc Tukey's HSD test).

(B) H_2O_2-triggered oxidation of persulfidated DES1 in guard cells. Total proteins extracted from *pMYB60:DES1-GFP des1* transgenic plant were subjected to the tag-switch assay after exposure to H_2O_2 at different concentrations for 1 hr. Two images of the same blot with different time of exposure are shown.

(D) Enhancement of ABA-induced DES1 persulfidation by DPI in guard cells. Total proteins extracted from *pMYB60:DES1-GFP des1* transgenic plants were subjected to the tag-switch assay after exposure to ABA at 10 μM for 30 min, with or without pretreatment of DPI at 10 μM for 2 hr.

(E) ABA- and H_2O_2-regulated persulfidation of DES1 in guard cells. Total proteins extracted from *pMYB60:DES1-GFP des1* and *pMYB60:DES1-GFP des1 rbohD* transgenic plants were subjected to the tag-switch assay after exposure to ABA treatment at 10 μM for 30 min.

(F and G) Reversible persulfidation and persulfide-oxidation of DES1-His recombinant protein. Purified DES1 recombinant protein was NaHS pretreated at 10 mM for 1 h, followed by dialysis and then treated with H_2O_2 at 10 uM for the indicated times (F), or H_2O_2 pretreamted at 10 uM for 1hr, followed by dialysis and treated with NaHS at 10 uM for the indicated times (G), and then subjected to a tag-switch assay for the analysis of the persulfidation level (DES1-SSH).

For *in vitro* assay, the persulfidated recombinant protein was detected by an anti-biotin antibody after the tag-switch labeling. CBB, Coomassie Brilliant Blue protein stain. IB, Immunoblotting. For *in vivo* assay, 4-week-old plants grown in the soil were treated and harvested at the indicated times. The persulfidated DES1-GFP protein in guard cells was detected by an anti-GFP antibody after tag-switch labeling and streptavidin purification. The bottom panels show that the total DES1-GFP used for the tag-switch assay as loading control. The numbers above the bottom panel indicate the relative abundance of the corresponding persulfidated protein compared with that of the control sample (1.00). Signals from two independent experiments were quantified.

Figure 3

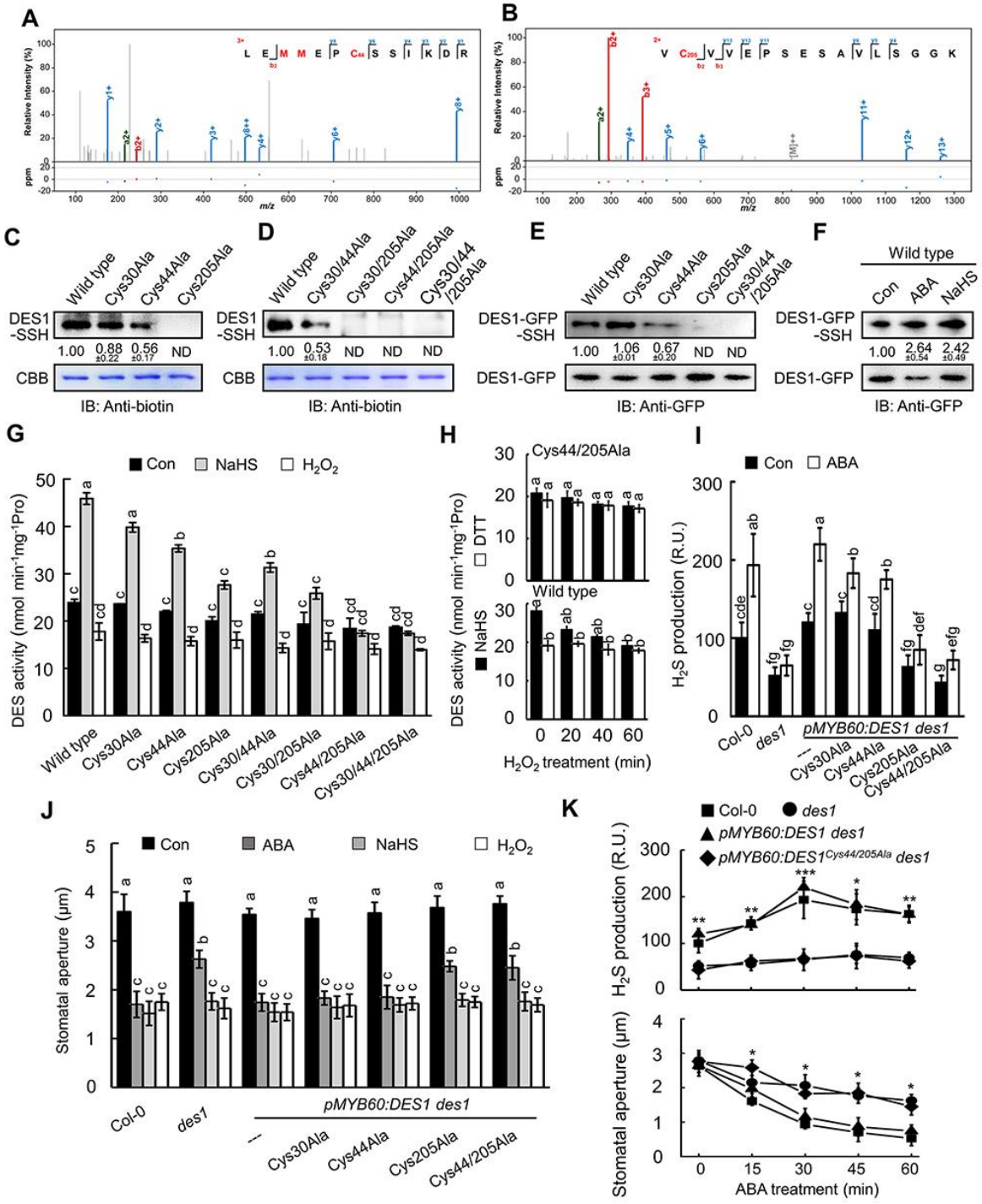

Figure 3 Persulfidation of DES1 on Cys44 and Cys205 Regulates ABA-Induced Stomatal Closure

(A and B) Fully annotated MS/MS spectra of IAM-derivatized DES1 peptides containing persulfided cysteines. Purified recombinant DES1 protein was treated with NaHS (1 mM for 1 hr), alkylated with iodoacetamide (IAM), and analyzed by LC-MS/MS. The localization of IAM-derivatized persulfides was unequivocally annotated according to the modification-specific b- or y-ions .

(C and D) *In vitro* persulfidation analysis of DES1 and mutant recombinant proteins by the tag-switch method. The persulfidated protein was detected by an anti-biotin antibody.

(E) *In vivo* persulfidation analysis of the mutated versions of DES1 protein. Total proteins from Arabidopsis protoplasts transiently expressed DES1 and its mutant derivatives fused to GFP were subjected to the tag-switch assay for the analysis of the level of persulfidation of different versions of DES1(DES1-SSH). The bottom panel shows the total DES1-GFP used for the tag-switch assay as loading control.

(F) Effect of ABA and NaHS on the persulfidation level of DES1 *in vivo*. Total proteins from Arabiodopsis protoplasts transiently expressed unmutated DES1 fused to GFP were treated with or without ABA (10 μM for 30 min) or NaHS (1 mM for 1 hr) before subjected to the tag-switch assay for the analysis of the level of persulfidation (DES1-SSH). The bottom panel shows the total DES1-GFP used for the tag-switch assay as loading control.

(G) DES enzyme activity of different versions of the DES1-His recombinant proteins in the presence or absence of NaHS or H_2O_2. Recombinant proteins were pretreated with either NaHS (10 μM) or H_2O_2 (10 μM) for 1hr. Con means untreated conditions. The data represent mean ± SD (*n* = 3) from three biological replicates. Bars denoted by the different letters were different significantly at P < 0.05 according to one-way ANOVA (post-hoc Tukey's HSD test).

(H) Reversibility of the enzyme activity of DES1-His recombinant protein (wildype) and its mutant derivative Cys44/205Ala. Recombinant proteins were pretreated with either NaHS (10 μM) or DTT (1 mM) for 1hr, followed by dialysis and then treated with the H_2O_2 (10 μM) at the indicated times. The data represent mean ± SD (*n* = 3) from three biological replicates. Different letters were different significantly at P < 0.05 according to one-way ANOVA (post-hoc Tukey's HSD test).

(I and J) Effects of ABA and NaHS on the guard cell H_2S production and stomatal closure of wild type, the *des1*, and the *des1* with different mutated varieties. H_2S production was monitored using the fluorescent dye 7-Azido-4-Methylcoumarin (AzMC). Epidermal strips of each line were pre-incubated for 3 hr in opening buffer (10 mM MES, pH 6.15, and 10 mM KCl) under light (120 μE $m^{-2}s^{-1}$) and loaded with AzMC (15 μM) for 40 min before washing in MES buffer three times for 15 min each. Subsequently, samples were treated for 30 min with ABA (10 μM), NaHS (100 μM) or H_2O_2 (10 μM), respectively. For (G), the value 100% corresponds to the fluorescence of wild type in control conditions. R.U., relative units. The corresponding stomatal aperture sizes were also measured. The data represent mean ± SD from three biological replicates (*n* ≥ 90 in each replicate). Bars denoted by the different letters were different significantly at *P* < 0.05 according to two-way ANOVA (post-hoc Tukey's HSD test).

(K) Stomatal closure and H_2S production rate of different plant lines under ABA treatment for the indicated times. Treatment and measurement details are described in Figure. 3I and J. The data represent mean ± SD from three biological replicates (*n* ≥ 90 in each replicate). Asterisks represent significant differences between *pMYB60:DES1 des1* and *pMYB60:DES1Cys44/205Ala des1* according to Student's t-test (*P < 0.05, **P < 0.01, ***P < 0.001).

4-week-old plants grown in the soil were treated and harvested at the indicated times. For the immunoblot, the numbers upon the bottom panels indicate the relative abundance of the corresponding persulfidated protein compared with that of the control sample (1.00). Signals from two independent experiments were quantified. CBB, Coomassie Brilliant Blue protein stain. IB, Immunoblotting. Wild type represents the unmutated version of DES1 protein.

Figure 4

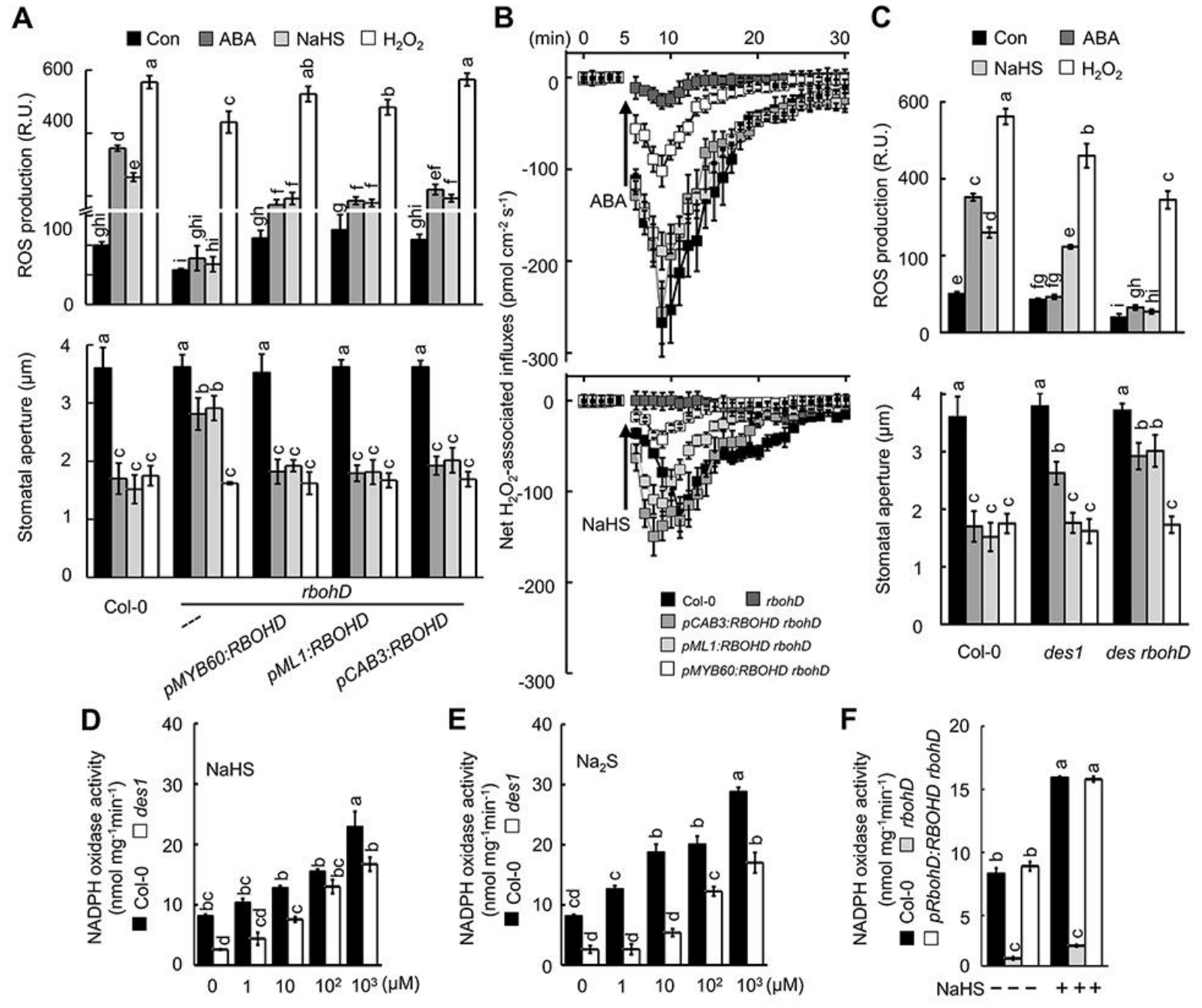

Figure 4. H_2S Requires RBOHD Activity for the Induction of Stomatal Closure

(A) ROS production in guard cells and stomatal responses of wild type, *rbohD*, and *rbohD* rescued lines. RBOHD was rescued by expressing RBOHD under the control of tissue-specific promoters, in which RBOHD was expressed in guard cells (*pMYB60: RBOHD*), epidermal (*pML1: RBOHD*), or mesophyll cells (*pCAB3: RBOHD*) individually. ROS production was monitored using florescent dye H_2DCFDA (upper panel). Epidermal strips of each line were pre-incubated for 3 hr in opening buffer (10 mM MES, pH 6.15, and 10 mM KCl) under light (120 μE m^{-2}s^{-1}) and loaded with H_2DCFDA (15 μM) for 15 min before washing in MES buffer three times for 15 min each. Subsequently, samples were treated for 1 hr with ABA (10 μM), NaHS (100 μM) or H_2O_2 (10 μM), respectively. The value 100% corresponds to the fluorescence of wild type (Col-0) in control conditions. R.U., relative units. The corresponding stomatal aperture sizes were also measured (lower panel). The data represent mean ± SD from three biological replicates (n ≥ 90 in each replicate). Bars denoted by the different letters were different significantly at $P < 0.05$ according to two-way ANOVA (post-hoc Tukey's HSD test).

(B) ABA- and NaHS-induced net H_2O_2 influxes in guard cells of *rbohD* and *pCAB3:RBOHD rbohD* plants. Leaves from 4-week-old plant were preincubated for 3 hr in opening buffer (10 mM MES, pH 6.15, and 10 mM KCl) under light (120 μE m^{-2}s^{-1}) and washed in MES buffer three times for 15 min each. The net H_2O_2 influxes were observed after ABA (10 μM) or NaHS (100 μM) treatment during the indicated times (n = 6)

(C) ROS production in guard cells and stomatal responses of wild type, *des1*, *des1 rbohD*, and *des1 rbohD* rescued lines. Treatment and measurement details are shown in Figure. 4A.

(D-F) Effects of sulfurating molecules on NADPH oxidase activity of wild type, *des1*, *rbohD*, and *rbohD* rescued line. For NADPH oxidase activity assay, the crude membrane extracts from each line (4-week-old) were extracted and treated with NaHS or Na_2S at indicated concentrations (0 - 1 mM; for F, NaHS at 100 μM) for 30 mins. NADPH oxidase activity was determined after dialysis. The data represent mean ± SD (n = 3) from three biological replicates. Different letters were different significantly at $P < 0.05$ according to two-way ANOVA (post-hoc Tukey's HSD test).

Figure 5

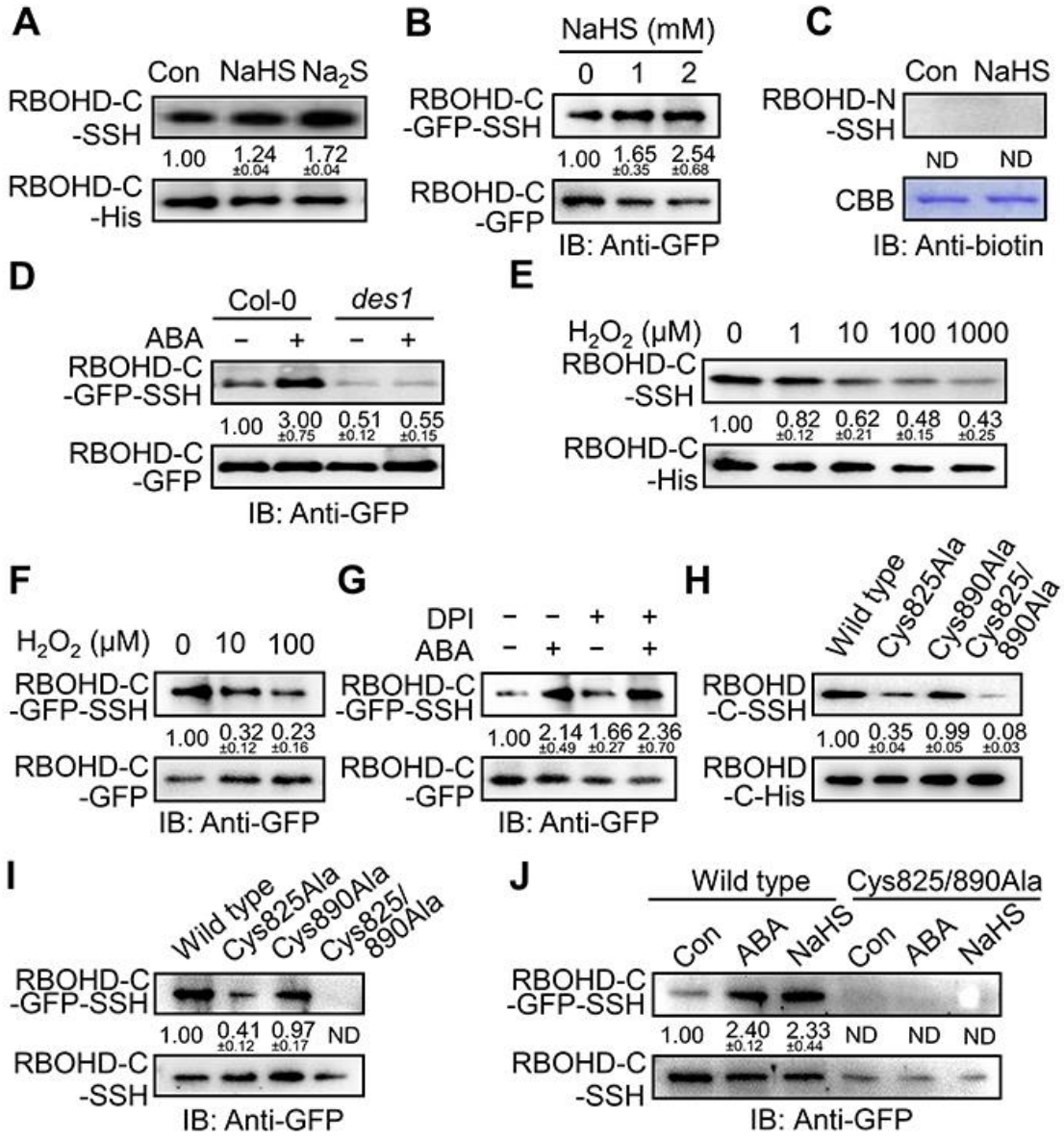

Figure 5. ABA-Induced Persulfidation of RBOHD at Cys825 and Cys890

(A) The C terminus of RBOHD is persulfidated in the presence or absence of two sulfurating molecules. RBOHD-C terminal recombinant protein was treated with NaHS or Na_2S at 1 mM for 1 hr before to be subjected to tag switch assay.

(B) Analysis of persulfidation of RBOHD-C terminal *in vivo*. Total proteins from Arabidopsis wild type protoplast transformed with *35S:RBOHD-C-GFP* were extracted and exposed to NaHS for 1 hr at the indicated concentrations, followed by the tag-switch assay.

(C) The N terminus of RBOHD is not persulfidated. RBOHD-N terminal recombinant protein was treated with NaHS 1 mM for 1 hr before to be subjected to tag switch assay.

(D) ABA-induced persulfidation of RBOHD-C terminal *in vivo*. Total proteins from Arabidopsis wild type (Col-0) and *des1* mutant protoplasts transformed with *35S:RBOHD-C-GFP* were extracted and treated with or without ABA at 10 μM for 30 min, followed by the subject to the tag-switch assay.

(E and F) H_2O_2-triggered persulfide-oxidation of the RBOHD-C terminal recombinant protein *in vitro* (E) or RBOHD-C-GFP protein *in vivo* (F). Samples were treated with H_2O_2 at indicated concentrations for 1 hr before to be subjected to the tag-switch assay.

(G) Enhancement of ABA-induced RBOHD-C-GFP persulfidation by DPI. Total proteins from Arabidopsis protoplast transformed with *35S:RBOHD-C-GFP* were subjected to the tag-switch assay after exposure to ABA at 10 μM for 30 min, with or without pretreatment of DPI at 10 μM for 2 hr.

(H-J) Persulfidation analysis of the C terminus of wild type and mutant RBOHD derivatives *in vitro* (H) and *in vivo* (I and J).

For *in vitro* assay, the persulfidated recombinant proteins were detected by an anti-biotin antibody after the tag-switch labeling. Proteins were detected by immunoblotting using an anti-his antibody served as a loading control. Con, control. CBB, Coomassie Brilliant Blue protein stain. For *in vivo* assay, total proteins from Arabidopsis protoplasts transiently expressed the RBOHD C terminus and its mutant derivatives fused to GFP were treated with or without ABA (10 μM for 30 min) or NaHS (1 mM for 1 hr) before to be subjected to the tag-switch assay and streptavidin purification. The persulfidated proteins were detected by an anti-GFP antibody. The bottom panels show the total GFP fused proteins used for the tag-switch assay as loading control. Wild type represents the unmutated version of RBOHD-C protein and Con means untreated conditions. The numbers above the bottom panels indicate the relative abundance of the corresponding persulfidated protein compared with that of the control sample (1.00). Signals from two independent experiments were quantified.

Figure 6

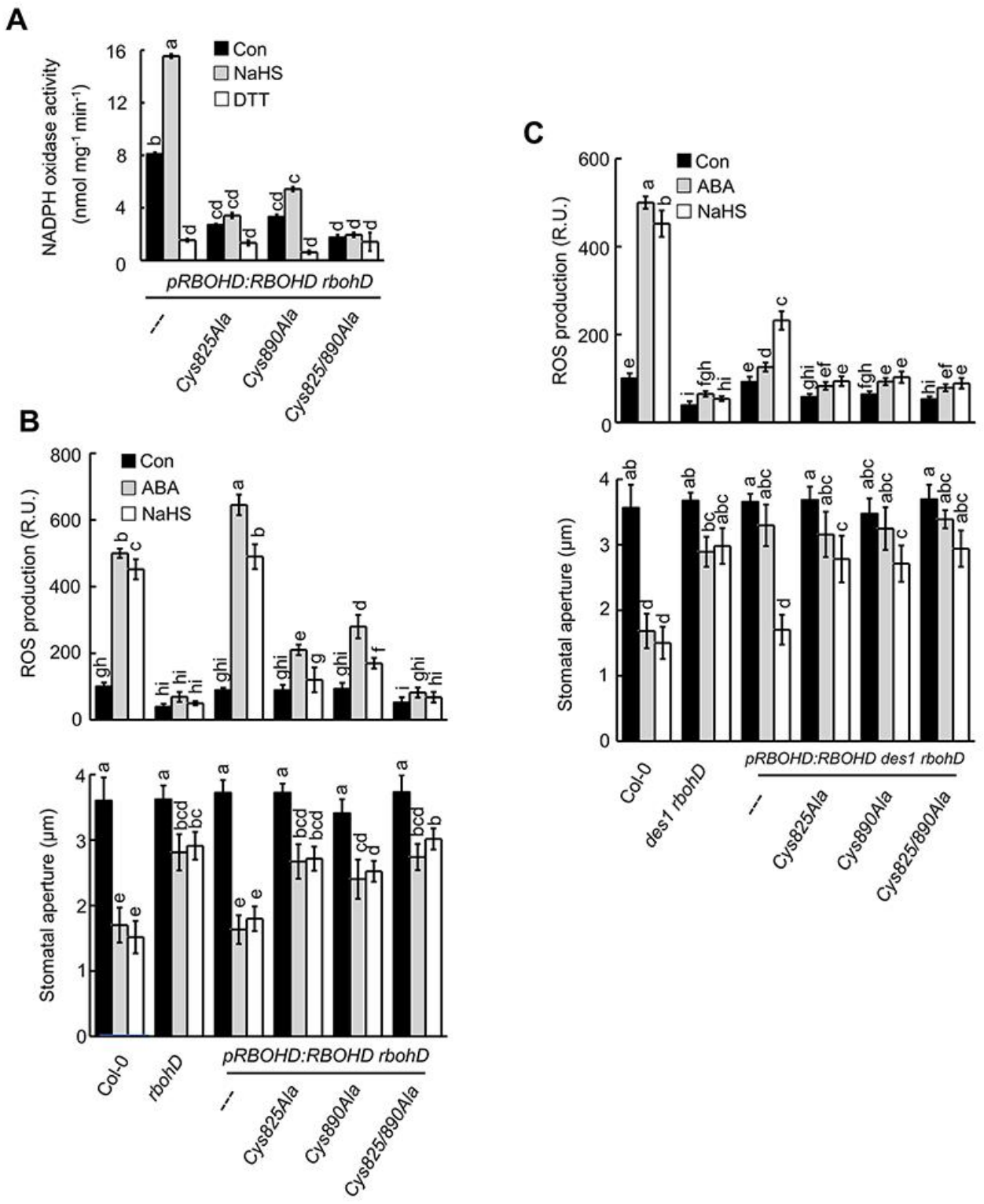

Figure 6. DES1-Triggered Persulfidation of RBOHD at C825 and C890 is Involved in ABA-Induced ROS Activation and Stomatal Closure.
(A) Effects of NaHS or DTT on the activity of NADPH oxidase of mutant *rbohD* plants expressing either a wild type RBOHD or Cys825Ala, Cys890Ala and Cys825/890Ala mutant derivatives driven by its native promoter. Treatment and measurement details are represented in Figure. 4D-F.
(B and C) Effects of ABA or NaHS on ROS production and stomatal closure of wild type (Col-0), *rbohD*, *des1 rbohD*, and lines expressing either a wild type RBOHD or Cys825Ala, Cys890Ala and Cys825/890Ala mutant derivatives driven by its native promoter. Treatment and measurement details are shown in Figure. 4A.

Figure 7

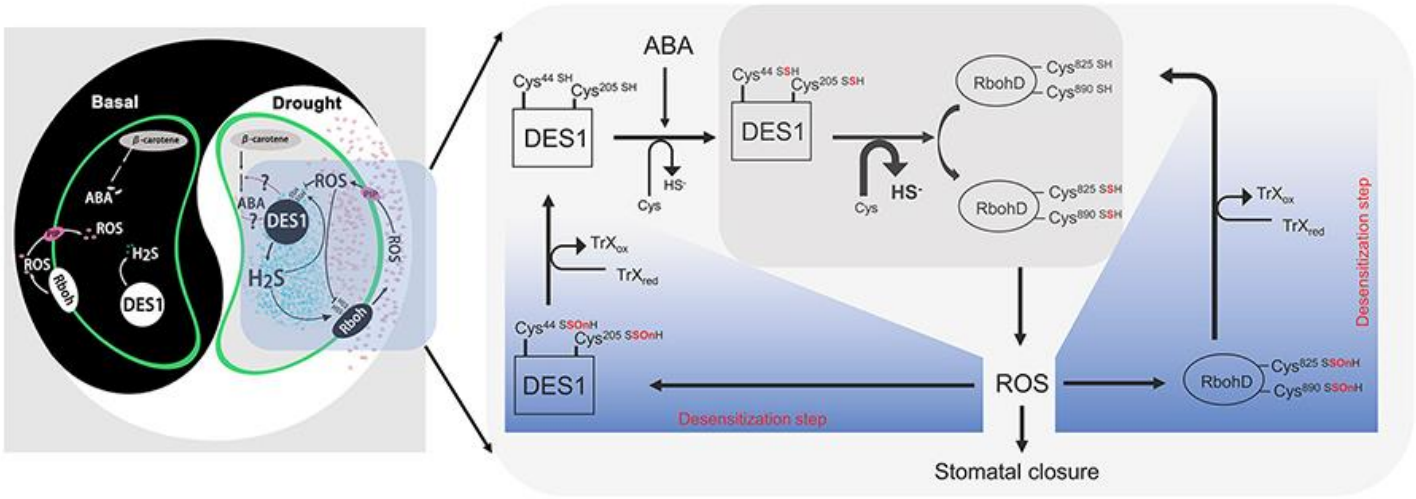

Figure 7. Working Model Shown in This Study. While drought stress signal was sensed by the plant, ABA was synthesized and triggered rapid and strong expression of DES1 in guard cells by unknown mechanism. Inducible DES1 expression can persulfide many downstream signaling proteins, including itself on Cys44 and Cys205, and leading to the amplification of guard cell H_2S signals. The inducible DES1/H_2S also persulfidates NADPH oxidase RBOHD on Cys825 and Cys890 to facilitate the rapid induction of ROS burst, which in turn causes stomatal closure. When ROS accumulates to high levels, it further causes persulfide-oxidation of RBOHD and DES1 (-SSO_nH), leading to ABA de-sensitivity. The oxidized persulfide (-SSO_nH) may subsequently be reduced to thiol group (-SH) by thioredoxin, which formed a feed-back prevention of ABA signaling continuously activated in guard cells.

Parsed Citations

Akter, S., L. Fu, Y. Jung, M. L. Conte, J. R. Lawson, W. T. Lowther, R. Sun, K. Liu, J. Yang and K. S. Carroll (2018). Chemical proteomics reveals new targets of cysteine sulfinic acid reductase. Nat Chem Biol 14, 995-1004.
Pubmed: Author and Title
Google Scholar: Author Only Title Only Author and Title

Álvarez, C., Calo, L., Romero, L.C., García, I., and Gotor, C. (2010). An O-acetylserine(thiol)lyase homolog with L-cysteine desulfhydrase activity regulates cysteine homeostasis in Arabidopsis. Plant Physiol. 152, 656-669.
Pubmed: Author and Title
Google Scholar: Author Only Title Only Author and Title

Anderson, A., Bothwell, J. H., Laohavisit, A., Smith, A. G., and Davies, J. M. (2011). Nox or not? Evidence for algal NADPH oxidases. Trends Plant Sci. 16, 579-581.
Pubmed: Author and Title
Google Scholar: Author Only Title Only Author and Title

Aroca, A., Benito, J.M., Gotor, C., and Romero, L.C. (2017a). Persulfidation proteome reveals the regulation of protein function by hydrogen sulfide in diverse biological processes in Arabidopsis. J. Exp. Bot. 68, 4915-4927.
Pubmed: Author and Title
Google Scholar: Author Only Title Only Author and Title

Aroca A, Schneider M, Scheibe R, Gotor C, Romero LC. (2017b). Hydrogen sulfide regulates the cytosolic/nuclear partitioning of glyceraldehyde-3-phosphate dehydrogenase by enhancing its nuclear localization. Plant and Cell Physiology 58, 983-992.
Pubmed: Author and Title
Google Scholar: Author Only Title Only Author and Title

Aroca, A., Gotor, C., Romero, L.C. (2018) Hydrogen sulfide signaling in plants: emerging roles of protein persulfidation. Front. Plant Sci. https://doi.org/10.3389/fpls.2018.01369.
Pubmed: Author and Title
Google Scholar: Author Only Title Only Author and Title

Aroca, A., Serna, A., Gotor, C., and Romero, L.C. (2015). S-sulfhydration: a cysteine posttranslational modification in plant systems. Plant Physiol. 168, 334-342.
Pubmed: Author and Title
Google Scholar: Author Only Title Only Author and Title

Batool, S., Uslu, V., Rajab, H., Ahmad, N., Waadt, R., Geiger, D., Malagoli, M., Xiang, C., Hedrich, R., Rennenberg, H., Herschbach, C., Hell, R., and Wirtz, M. (2018). Sulfate is incorporated into cysteine to trigger ABA produciton and stomatal closure. Plant Cell 30, 2973-2987.
Pubmed: Author and Title
Google Scholar: Author Only Title Only Author and Title

Bauer, H., Ache, P., Lautner, S., Fromm, J., Hartung, W., Al-Rasheid, K., Sonnewald, S., Sonnewald, U., Kneitz, S., Lachmann, N., Mendel, R., Bittner, F., Hetherington, A., and Hedrich, R. (2013). The stomatal response to reduced relative humidity requires guard cell-autonomous ABA synthesis. Curr. Biol. 23, 53-57.
Pubmed: Author and Title
Google Scholar: Author Only Title Only Author and Title

Bernula, P., Crocco, C.D., Arongaus, A.B., Ulm, R., Nagy, F., and Viczián, A. (2017). Expression of the UVB8 photoreceptor in different tissues reveals tissue-autonomous features of UV-B signalling. Plant Cell Environ. 40, 1104-1114.
Pubmed: Author and Title
Google Scholar: Author Only Title Only Author and Title

Blatt, M. (2010). Cellular signaling and volume control in stomatal movements in plants. Annu. Rev. Cell Dev.Biol. 16. 221-241.
Pubmed: Author and Title
Google Scholar: Author Only Title Only Author and Title

Bogdandi, V., T. Ida, T. R. Sutton, C. Bianco, T. Ditroi, G. Koster, H. A. Henthorn, M. Minnion, J. P. Toscano, A. van der Vliet, M. D. Pluth, M. Feelisch, J. M. Fukuto, T. Akaike and P. Nagy (2019). Speciation of reactive sulfur species and their reactions with alkylating agents: do we have any clue about what is present inside the cell? Br J Pharmacol. 176, 646-670.
Pubmed: Author and Title
Google Scholar: Author Only Title Only Author and Title

Boursiac, Y., Léran, S., Corratgéfaillie, C., Gojon, A., Krouk, G., and Lacombe, B. (2013). ABA transport and transporters. Trends Plant Sci. 18, 325-333.
Pubmed: Author and Title
Google Scholar: Author Only Title Only Author and Title

Bright, J., Desikan, R., Hancock, J.T., Weir, I.S., and Neill, S.J. (2010). ABA-induced no generation and stomatal closure in Arabidopsis are dependent on H2O2 synthesis. Plant J. 45, 113-122.
Pubmed: Author and Title
Google Scholar: Author Only Title Only Author and Title

Cao, M.J., Wang, Z., Zhao, Q., Mao, J.L., Speiser, A., Wirtz, M., Hell, R., Zhu, J., and Xiang, C. (2014). Sulfate availability affects ABA levels and germination response to ABA and salt stress in Arabidopsis thaliana. Plant J. 77, 604-615.
Pubmed: Author and Title
Google Scholar: Author Only Title Only Author and Title

Chater, C., Peng, K., Movahedi, M., Dunn, J.A., Walker, H.J., and Liang, Y.K. (2015). Elevated CO2-induced responses in stomata require ABA and ABA signaling. Curr. Biol. 25, 2709-2716.
Pubmed: Author and Title
Google Scholar: Author Only Title Only Author and Title

Chen, D., Cao, Y., Li, H., Kim, D., Ahsan, N., Thelen, J., and Stacey, G. (2017). Extracellular ATP elicits DORN1-mediated RBOHD phosphorylation to regulate stomatal aperture. Nat. Comm. 8, 2265-2677.
Pubmed: Author and Title
Google Scholar: Author Only Title Only Author and Title

Chi, H., C. Liu, H. Yang, W. F. Zeng, L. Wu, W. J. Zhou, R. M. Wang, X. N. Niu, Y. H. Ding, Y. Zhang, Z. W. Wang, Z. L. Chen, R. X. Sun, T. Liu, G. M. Tan, M. Q. Dong, P. Xu, P. H. Zhang and S. M. He (2018). Comprehensive identification of peptides in tandem mass spectra using an efficient open search engine. Nat Biotechnol. 36, 1059-1061.
Pubmed: Author and Title
Google Scholar: Author Only Title Only Author and Title

Christmann, A., Weiler, E.W., Steudle, E., and Grill, E. (2007). A hydraulic signal in root-to-shoot signalling of water shortage. Plant J. 52, 167-174.
Pubmed: Author and Title
Google Scholar: Author Only Title Only Author and Title

Corpas, F.J., González-Gordo, S., Cañas, A., and Palma, J.M. (2019). Nitric oxide (NO) and hydrogen sulfide (H2S) in plants: Which is first? J. Exp. Bot. https://doi.org/10.1093/jxb/erz031.
Pubmed: Author and Title
Google Scholar: Author Only Title Only Author and Title

Desikan, R., Cheung, M.K., Bright, J., Henson, D., Hancock, J.T., and Neill, S.J. (2004). ABA, hydrogen peroxide and nitric oxide signalling in stomatal guard cells. J. Exp. Bot. 55, 205-212.
Pubmed: Author and Title
Google Scholar: Author Only Title Only Author and Title

Du, X.Z, Jin, Z.P., Zhang, L.P., Liu, X., Yang, G.D., and Pei, Y.X. (2019). H2S is involved in ABA-mediated stomatal movement through MPK4 to alleviate drought stress in Arabidopsis thaliana. Plant Soil. 435, 295-307.
Pubmed: Author and Title
Google Scholar: Author Only Title Only Author and Title

Filipovic, M.R., and Jovanović, V.M. (2017). More than just an intermediate: hydrogen sulfide signalling in plants. J. Exp. Bot. 68, 4733-4736.
Pubmed: Author and Title
Google Scholar: Author Only Title Only Author and Title

Filipovic, M.R., Zivanovic, J., Alvarez, B., and Banerjee, R. (2018). Chemical biology of H2S signaling through persulfidation. Chem. Rev. 118, 1253-1337.
Pubmed: Author and Title
Google Scholar: Author Only Title Only Author and Title

Fu, L., K. Liu, J. He, C. Tian, X. Yu and J. Yang (2019). Direct Proteomic Mapping of Cysteine Persulfidation. Antioxid Redox Signal. Doi:10.1089/ars.2019.7777
Pubmed: Author and Title
Google Scholar: Author Only Title Only Author and Title

Garcia-Mata, C., and Lamattina, L. (2010). Hydrogen sulphide, a novel gasotransmitter involved in guard cell signalling. New Phytol. 188, 977-984.
Pubmed: Author and Title
Google Scholar: Author Only Title Only Author and Title

Gilroy, S., Suzuki, N., Miller, G., Choi, W.G., Toyota, M., Devireddy, A.R., and Mitter, R. (2014) A tidal wave of signals: calcium and ROS at the forefront of rapid systemic signaling. Trends in Plant Sci. 19, 623-630.
Pubmed: Author and Title
Google Scholar: Author Only Title Only Author and Title

Gotor, C., Garcia, I., Aroca, A., Laureano-Marin, A.M., Arenas-Alfonseca, L., Jurado-Flores, A., Moreno, I., and Romero, L.C. (2019) Signaling by hydrogen sulfide and cyanide through posttranslational modification. J Exp Bot. 70, 4251-4265.
Pubmed: Author and Title
Google Scholar: Author Only Title Only Author and Title

Guo, H.M., Xiao, T.Y., Zhou, H., Xie, Y.J., and Shen, W.B. (2016). Hydrogen Sulfide, a versatile regulator of environmental stress in Plants. Acta. Physiol. Plant 38, 1-13.
Pubmed: Author and Title
Google Scholar: Author Only Title Only Author and Title

Guo, H.M., Zhou, H., Zhang, J., Guan, W.X., Xu, S., Shen, W.B., Xu, G.H., Xie, Y.J., and Foyer, C.H. (2017). L-cysteine desulfhydrase-related H2S production is involved in OsSE5-promoted ammonium tolerance in roots of Oryza sativa. Plant Cell & Environ, 2017, 40: 1777-1790
Pubmed: Author and Title
Google Scholar: Author Only Title Only Author and Title

Hancock, J. (2019). Considerations of the importance of redox state for reactive nitrogen species action. J Exp. Bot. https://doi.org/10.1093/jxb/erz067.
Pubmed: Author and Title
Google Scholar: Author Only Title Only Author and Title

Hauser, F., Li, Z., Waadt, R., and Schroeder, J.I. (2017). Snapshot: Abscisic Acid signaling. Cell 171, 1708-1708.
Pubmed: Author and Title
Google Scholar: Author Only Title Only Author and Title

Honda, K., Yamada, N., Yoshida, R., Ihara, H., Sawa, T., and Akaike, T. (2015). 8-mercapto-cyclic GMP mediates hydrogen sulfide-induced stomatal closure in Arabidopsis. Plant Cell Physiol. 56, 1481-1489.
Pubmed: Author and Title
Google Scholar: Author Only Title Only Author and Title

Huang, J., P. Willems, B. Wei, C. Tian, R. B. Ferreira, N. Bodra, S. A. Martinez Gache, K. Wahni, K. Liu, D. Vertommen, K. Gevaert, K. S. Carroll, M. Van Montagu, J. Yang, F. Van Breusegem and J. Messens (2019). Mining for protein S-sulfenylation in Arabidopsis uncovers redox-sensitive sites. Proc Natl Acad Sci U S A 116: 21256-21261.
Pubmed: Author and Title
Google Scholar: Author Only Title Only Author and Title

Jin, Z., Xue, S., Luo, Y., Tian, B., Fang, H., Li, H., and Pei, Y. (2013). Hydrogen sulfide interacting with abscisic acid in stomatal regulation responses to drought stress in Arabidopsis. Plant Physiol. Biochem. 62, 41-46.
Pubmed: Author and Title
Google Scholar: Author Only Title Only Author and Title

Kim, T.H., Böhmer, M., Hu, H.H., Nishimurab, N., and Schroeder, J. (2010). Guard cell signal transduction network: advances in understanding abscisic acid, CO2, and Ca2+ signaling. Annu. Rev. Plant Biol. 61, 561-591.
Pubmed: Author and Title
Google Scholar: Author Only Title Only Author and Title

Kirchenbauer, D., Viczian, A., Adam, E., Hegedus, Z., Klose, C., Leppert, M., and Nagy, F. (2016). Characterization of photomorphogenic responses and signaling cascades controlled by phytochrome-A expressed in different tissues. New Phytol. 211, 584-598.
Pubmed: Author and Title
Google Scholar: Author Only Title Only Author and Title

Kuromori, T., Sugimoto, E., Shinozaki, K. (2014) Intertissue signal transfer of abscisic acid from vascular cells to guard cells. Plant Physiol. 164, 1587-1592.
Pubmed: Author and Title
Google Scholar: Author Only Title Only Author and Title

Kwak, J.M., Mori, I.C., Pei, Z.M., Leonhardt, N., Torres, M.A., Dangl, J.L., Bloom, R.E., Bodde, S., Jones, J.D.G., and Schroeder J.I. (2003). NADPH oxidase AtrbohD and AtrbohF genes function in ROS-dependent ABA signaling in Arabidopsis. Embo J. 22, 2623-2633.
Pubmed: Author and Title
Google Scholar: Author Only Title Only Author and Title

Lai, D.W., Mao, Y., Zhou, H., Li, F., Wu, M.Z., Zhang, J., He, Z.Y., Cui, W.T., and Xie, Y.J. (2014) Endogenous hydrogen sulfide enhances salt tolerance by coupling the reestablishment of redox homeostasis and preventing salt-induced K+-loss in seedlings of Medicago sativa. Plant Sci, 205, 117-129.
Pubmed: Author and Title
Google Scholar: Author Only Title Only Author and Title

Laureano-Marín, A.M., García, I., Romero, L.C., Gotor, C. (2014). Assessing the transcriptional regulation of L-CYSTEINE DESULFHYDRASE 1 in Arabidopsis thaliana. Front Plant Sci 5:683.
Pubmed: Author and Title
Google Scholar: Author Only Title Only Author and Title

Li, J., Chen, S., Wang, X., Shi, C., Liu, H., Yang, J., Shi, W., Guo, J., and Jia, H. (2018). Hydrogen sulfide disturbs actin polymerization via S-sulfhydration resulting in stunted root hair growth. Plant Physiol. 178, 936-949.
Pubmed: Author and Title
Google Scholar: Author Only Title Only Author and Title

Ma, D., Ding, H., Wang, C., Qin, H., Han, Q., Hou, J., Lu, H., Xie, Y., and Guo, T. (2016). Alleviation of drought stress by hydrogen sulfide is partially related to the abscisic acid signaling pathway in wheat. PLoS One 9, e0163082.
Pubmed: Author and Title
Google Scholar: Author Only Title Only Author and Title

Magnani, F., Nenci, S., Millana, F.E., Ceccon, M., Romero, E., and Fraaije, M.W. (2017). Crystal structures and atomic model of NADPH

oxidase. Proc. Natl. Acad. Sci. USA 114, 6764-6769.
Pubmed: Author and Title
Google Scholar: Author Only Title Only Author and Title

Marino, D., Dunand, C., Puppo, A., and Pauly, N. (2012). A burst of plant NADPH oxidases. Trends Plant Sci. 17, 9-15.
Pubmed: Author and Title
Google Scholar: Author Only Title Only Author and Title

Miller, G., Schlauch, K., Tam, R., Cortes, D., Torres, M.A., Shulaev, V., and Mittler, D.R. (2009). The plant NADPH oxidase RBOHD mediates rapid systemic signaling in response to diverse stimuli. Sci. Signal. 2, ra45.
Pubmed: Author and Title
Google Scholar: Author Only Title Only Author and Title

Mittler, R., Vanderauwera, S., Suzuki, N., Miller, G., Tognetti, V.B., Vandepoele, K., Gollery, M., Shulaev, V., Van Breusegem, F. (2011). ROS signaling: the new wave? Trends in Plant Sci. 16, 300-309.
Pubmed: Author and Title
Google Scholar: Author Only Title Only Author and Title

Nambara, E., and Marion-Poll, A. (2005). Abscisic acid biosynthesis and catabolism. Annu. Rev. Plant Biol. 56,165-85.
Pubmed: Author and Title
Google Scholar: Author Only Title Only Author and Title

Nühse, T.S., Bottrill, A.R., Jones, A.M.E., and Peck, S.C. (2007). Quantitative phosphoproteomic analysis of plasma membrane proteins reveals regulatory mechanisms of plant innate immune responses. Plant J. 51, 931-947.
Pubmed: Author and Title
Google Scholar: Author Only Title Only Author and Title

Ogasawara, Y., Kaya, H., Hiraoka, G., Yumoto, F., Kimura, S., Kadota, Y., Hishinuma, H., Senzaki, E., Yamagoe, S., Nagata, K., Nara, M., Suzuki, K., Tanokura, M., Kuchitsu, K. (2008). Synergistic activation of the Arabidopsis NADPH oxidase AtrbohD by Ca2+ and phosphorylation. J. Biol. Chem. 283, 8885–8892.
Pubmed: Author and Title
Google Scholar: Author Only Title Only Author and Title

Palde, P.B., and Carroll, K.S. (2015). A universal entropy-driven mechanism for thioredoxin-target recognition. Proc Natl Acad Sci U S A 112, 7960-7965.
Pubmed: Author and Title
Google Scholar: Author Only Title Only Author and Title

Papanatsiou, M., Scuffi, D., Blatt, M.R., and García-Mata, C. (2015). Hydrogen sulfide regulates inward-rectifying k+ channels in conjunction with stomatal closure. Plant Physiol. 168, 29-35.
Pubmed: Author and Title
Google Scholar: Author Only Title Only Author and Title

Paul, B.D., and Snyder, S.H. (2012). H2S signalling through protein sulfhydration and beyond. Nat. Rev. Mol. Cell Biol. 13, 499-507.
Pubmed: Author and Title
Google Scholar: Author Only Title Only Author and Title

Scuffi, D., Alvarez, C., Laspina, N., Gotor, C., Lamattina, L., and Garcia-Mata, C. (2014). Hydrogen sulfide generated by L-cysteine desulfhydrase acts upstream of nitric oxide to modulate abscisic acid-dependent stomatal clsoure. Plant Physiol. 166, 2065-2076.
Pubmed: Author and Title
Google Scholar: Author Only Title Only Author and Title

Scuffi, D., Nietzel, T., Fino, L.M.D., Meyer, A.J., Lamattina, L., Schwarzländer, M., Laxalt, A.M., and García-Mata, C. (2018). Hydrogen sulfide increases production of NADPH oxidase-dependent hydrogen peroxide and phospholipase D-derived phosphatidic acid in guard cell signaling. Plant Physiol. 176, 2532-2542.
Pubmed: Author and Title
Google Scholar: Author Only Title Only Author and Title

Sen, N., Paul, B.D., Gadalla, M.M., Mustafa, A.K., Sen, T., and Xu, R. (2012). Hydrogen sulfide-linked sulfhydration of NF-κB mediates its antiapoptotic actions. Mol. Cell 45, 13-24.
Pubmed: Author and Title
Google Scholar: Author Only Title Only Author and Title

Sirichandra, C., Gu, D., Hu, H.C., Davanture, M., Lee, S., Djaoui, M., Valot, B., Zivy, M., Leung, J., Merlot, S., and Kwak, J. (2009). Phosphorylation of the Arabidopsis AtrbohF NADPH oxidase by OST1 protein kinase. FEBS Lett. 583, 2982-2986.
Pubmed: Author and Title
Google Scholar: Author Only Title Only Author and Title

Shevchenko, A., H. Tomas, J. Havlis, J. V. Olsen and M. Mann (2006). In-gel digestion for mass spectrometric characterization of proteins and proteomes. Nat Protoc 1: 2856-2860.
Pubmed: Author and Title
Google Scholar: Author Only Title Only Author and Title

Shen. J., Su. Y., Zhou. C., Zhang. F., Zhou. H., Liu. X., Wu. D.L., Yin. X.C., Xie. Y.J., Yuan. X.X. (2019) A putative rice L-cysteine desulfhydrase encodes a true L-cysteine synthase that regulates plant cadmium tolerance. Plant Growth Regul, doi: 10.1007/s10725-

019-00528-9.
Pubmed: Author and Title
Google Scholar: Author Only Title Only Author and Title

Smirnoff, N., and Arnaud, D. (2019). Hydrogen peroxide metabolism and functions in plants. New Phytol. 221, 1197-1214.
Pubmed: Author and Title
Google Scholar: Author Only Title Only Author and Title

Song, Y., Miao, Y., and Song, C.P. (2014). Behind the scenes: the roles of reactive oxygen species in guard cells. New Phytol. 201, 1121-1140.
Pubmed: Author and Title
Google Scholar: Author Only Title Only Author and Title

Suzuki, N., Miller, G., Morales, J., Shulaev, V., Torres, M.A., and Mittler, R. (2011). Respiratory burst oxidases: the engines of ROS signaling. Curr. Opin. Plant Biol. 14, 691-699.
Pubmed: Author and Title
Google Scholar: Author Only Title Only Author and Title

Tan, B.C., Joseph, L.M., Deng, W.T., Liu, L.J., Li, Q.B., Cline, K., McCarty, D.R. (2003) Molecular characterization of the Arabidopsis nine-cis expoxycarotenoid dioxygenase gene family. Plant J. 35, 44-56.
Pubmed: Author and Title
Google Scholar: Author Only Title Only Author and Title

Vandiver, M., Paul, B., Xu, R., Karuppagounder, K., Rao, F., Snowman, A., Ko, H., Lee, Y., Dawson, V., Dawson, T., Sen, N., and Snyder, S. (2013) Sulfhydration mediates neuroprotective actions of parkin. Nat Comm. 4, 1626
Pubmed: Author and Title
Google Scholar: Author Only Title Only Author and Title

Wang, P., and Song, C.P. (2008). Guard-cell signalling for hydrogen peroxide and abscisic acid. New Phytol. 178, 703-718.
Pubmed: Author and Title
Google Scholar: Author Only Title Only Author and Title

Xie, Y.J., Zhang, C., Lai, D.W., Sun, Y., Samma, M.K., Zhang, J., and Shen, W.B. (2014) Hydrogen sulfide delays GA-triggered programmed cell death in wheat aleurone layers by the modulation of glutathione homeostasis and heme oxygenase-1 expression. J Plant Physiol 171, 53-62.
Pubmed: Author and Title
Google Scholar: Author Only Title Only Author and Title

Xie, Y.J., Lai, D.W., Mao, Y., Zhang, W., Shen, W.B., and Guan, R.Z. (2013) Molecular cloning, characterization and expression analysis of a novel gene encoding L-cysteine desulfhydrase from Brassica napus. Mol Biotechnol, 54, 737-746.
Pubmed: Author and Title
Google Scholar: Author Only Title Only Author and Title

Yun, B.W., Feechan, A., Yin, M.H., Saidi, N.B.B., Le, B.T., Yu, M., Moore, J.W., Kang, J.G., Kwon, E., Spoel, S.H., Pallas, J.A., and Loake, G.J. (2011). S-nitrosylation of NADPH oxidase regulates cell death in plant immunity. Nature 478, 264-268.
Pubmed: Author and Title
Google Scholar: Author Only Title Only Author and Title

Zhang, J., Zhou, M.J., Ge, Z.L., Shen, J., Zhou, C., Gotor, C., Romero, L.C., Duan, X.L., Liu, X., Wu, D.L., Yin, X.C., and Xie, Y.J. (2019) ABA-triggered guard cell L-cysteine desulfhydrase function and in situ H2S production contributes to heme oxygenase-modulated stomatal closure. Plant Cell & Environ, doi: 10.1111/pce.13685
Pubmed: Author and Title
Google Scholar: Author Only Title Only Author and Title

Zhu J. (2016). Abiotic stress signaling and responses in plants. Cell 167, 313-324.
Pubmed: Author and Title
Google Scholar: Author Only Title Only Author and Title

Persulfidation-based Modification of Cysteine Desulfhydrase and the NADPH Oxidase RBOHD Controls Guard Cell Abscisic Acid Signaling

Jie Shen, Jing Zhang, Mingjian Zhou, Heng Zhou, Beimi Cui, Cecilia Gotor, Luis C. Romero, Ling Fu, Jing Yang, Christine H. Foyer, Qiaona Pan, Wenbiao Shen and Yanjie Xie

Plant Cell; originally published online February 5, 2020;
DOI 10.1105/tpc.19.00826